Cover Picture: Tropospheric Aqueous-Phase Free-Radical Chemistry: Radical Sources, Spectra, Reaction Kinetics and Prediction Tools (ChemPhysChem 18/2010)

ARTICLE *in* CHEMPHYSCHEM · DECEMBER 2010

Impact Factor: 3.42 · DOI: 10.1002/cphc.201000533 · Source: PubMed

CHEMPHYSCHEM

DOI: 10.1002/cphc.201000533

Tropospheric Aqueous-Phase Free-Radical Chemistry: Radical Sources, Spectra, Reaction Kinetics and Prediction Tools

Hartmut Herrmann,* Dirk Hoffmann, Thomas Schaefer, Peter Bräuer, and Andreas Tilgner[a]

Dedicated to our friends and colleagues Philippe Mirabel, Robert Lesclaux and Georges LeBras

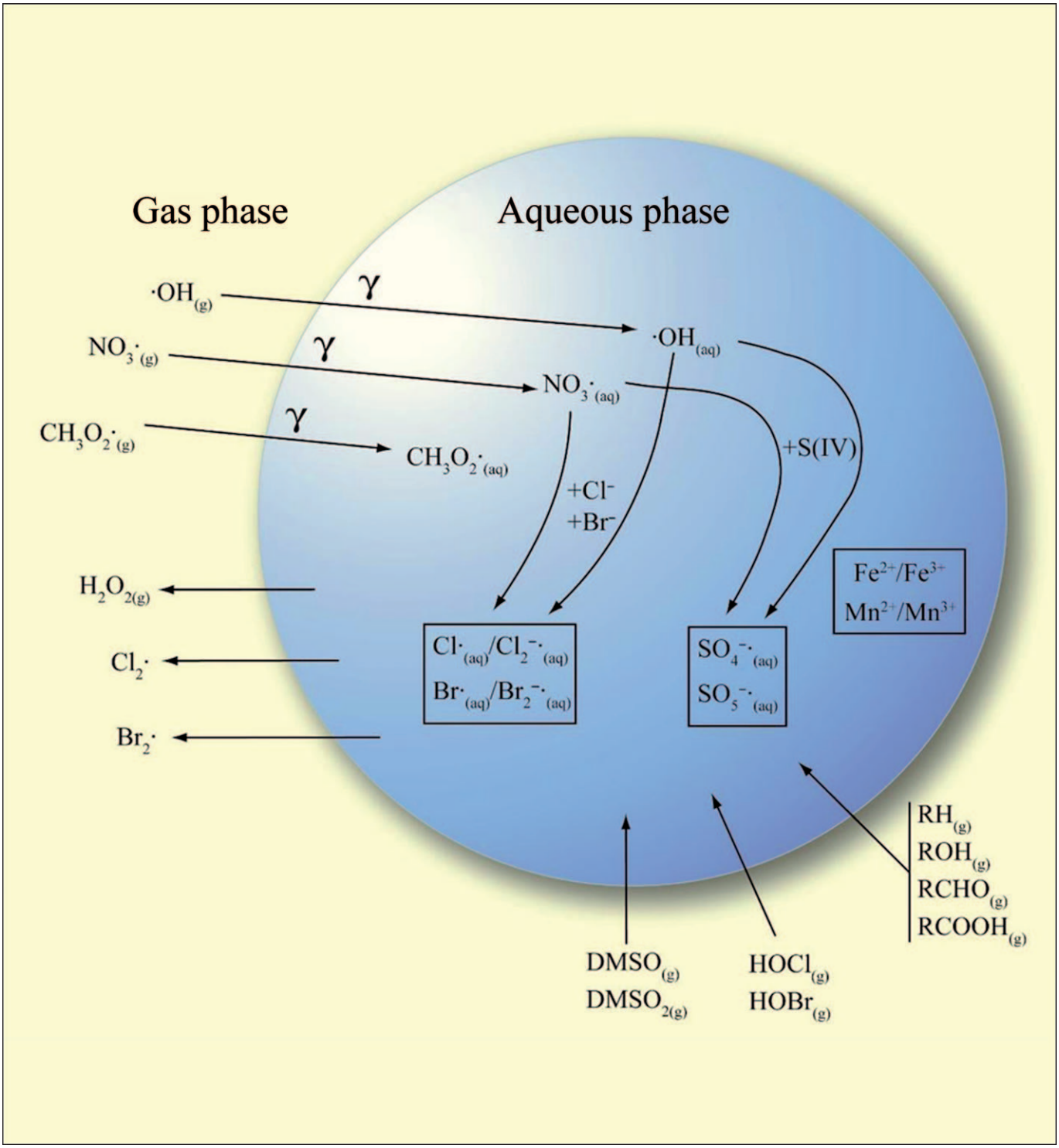

The most important radicals which need to be considered for the description of chemical conversion processes in tropospheric aqueous systems are the hydroxyl radical (OH), the nitrate radical (NO_3) and sulphur-containing radicals such as the sulphate radical (SO_4^-). For each of the three radicals their generation and their properties are discussed first in the corresponding sections. The main focus herein is to summarize newly published aqueous-phase kinetic data on OH, NO_3 and SO_4^- radical reactions relevant for the description of multiphase tropospheric chemistry. The data compilation builds up on earlier datasets published in the literature. Since the last review in 2003 (H. Herrmann, *Chem. Rev.* **2003**, *103*, 4691–4716) more than hundred new rate constants are available from literature. In case of larger discrepancies between novel and already published rate constants the available kinetic data for these reactions are discussed and recommendations are provided when possible. As many OH kinetic data are obtained by means of the thiocyanate (SCN^-) system in competition kinetic measurements of OH radical reactions this system is reviewed in a subchapter of this review. Available rate constants for the reaction sequence following the reaction of $OH + SCN^-$ are summarized. Newly published data since 2003 have been considered and averaged rate constants are calculated. Applying competition kinetics measurements usually the formation of the radical anion $(SCN)_2^-$ is monitored directly by absorption measurements. Within this subchapter available absorption spectra of the $(SCN)_2^-$ radical anion from the last five decades are presented. Based on these spectra an averaged $(SCN)_2^-$ spectrum was calculated. In the last years different estimation methods for aqueous phase kinetic data of radical reactions have been developed and published. Such methods are often essential to estimate kinetic data which are not accessible from the literature. Approaches for rate constant prediction include empirical correlations as well as structure activity relationships (SAR) either with or without the usage of quantum chemical descriptors. Recently published estimation methods for OH, NO_3 and SO_4^- radical reactions in aqueous solution are finally summarized, compared and discussed.

1. Introduction

Atmospheric research over the last three decades has shown that the atmosphere cannot be described as a pure gas-phase reactor, but that it involves a wide variety of particles which foster heterogeneous and multiphase chemical conversions coupled to the gas-phase reactions. Particles can consist of inorganic or organic material and exist as dry or wet, that is, aqueous particles including cloud droplets, as well as internal mixtures of the different types. Naturally, all of the different particle types provide media for chemical reactions and strongly interact with their surrounding phases by mass transfer as well as interfacial reactions. One important class of particle-phase chemical reactions consists of reactions occurring in the aqueous phase, which is found in deliquescent particles, activated particles and the droplets of clouds, fog and rain. Tropospheric aerosol particles will under many circumstances carry liquid water and hence particle chemistry at not too low relative humidities will to a large extent be explained by reactions occurring in aqueous solution. The scope of the present article is to treat reactions of the most important radicals OH, NO_3 and SO_4^- in the tropospheric aqueous phase. Effects and details of such tropospheric aqueous phase chemistry can be assessed by mechanism treating of such processes and the reader is referred here to the development of the chemical aqueous phase radical mechanism (CAPRAM).[1,2]

Herein, we summarize and discuss kinetic data of atmospherically relevant free radical reactions in aqueous solution. As in other complex systems, the hydroxyl radical is also most important in atmospheric aqueous phase chemistry and hence a major part of the present contribution is dealing with OH. The most prominent system to generate OH photochemically, that is, the photolysis of H_2O_2, will be reviewed as well as the UV-absorption spectrum of OH in aqueous solution. Due to the nature of the UV absorption of OH in water, competition kinetics is often the method of choice to investigate OH radical reaction in the aqueous phase and hence the SCN^- competition kinetics system is reviewed as its application is wide-spread.

In further chapters, mainly kinetic data for the nitrate (NO_3) radical and the sulphate radical anion (SO_4^-) are reviewed together with additional recent information available for these radicals.

The presented dataset builds up on the data compilation from Buxton in 1988,[3] Neta in 1988,[4] Herrmann and Zellner in 1998,[5] the NIST Solution Kinetics Database 3.0 of 1998,[6] and the review by Herrmann in 2003.[7] Since the appearance of this latter review article in 2003[7] hundreds of new kinetic data were reported in the literature, describing free radical reactions in aqueous solution. Reaction rate constants summarized in the following chapters are restricted to reactions of potential atmospheric interest only and do not necessarily reflect all the published aqueous phase kinetic data since 2003.

Data summarized in the following includes both novel data as well as new measurements of already published data. In case of large deviations, that is, here larger than a factor of two, between the novel and the existing rate constants the kinetic data are compared and discussed.

As it will be impossible to measure all free radical rate constant to construct a complex multiphase mechanism covering a bigger fraction of organic chemistry for the condensed phase, there is a clear need for estimation methods for radical reaction rate constants in aqueous solution. Of course, such

[a] *Prof. H. Herrmann, Dr. D. Hoffmann, T. Schaefer, P. Bräuer, Dr. A. Tilgner*
Chemistry Department
Leibniz-Institute for Tropospheric Research
Permoserstr. 15, 04318 Leipzig (Germany)
Fax: (+49) 3412352325
E-mail: herrmann@tropos.de

Supporting information for this article is available on the WWW under http://dx.doi.org/10.1002/cphc.201000533.

methods are also of interest for other fields of oxidative chemistry, that is, surface water chemistry, groundwater chemistry and water treatment technologies.

Methods for rate constant prediction which are presently available from recent studies will be reviewed and their performance evaluated.

2. The Hydroxyl (OH) Radical

The hydroxyl radical is of particular importance for chemical conversion processes in the tropospheric multiphase system being the dominant while most reactive oxidant. OH radical reactions trigger important degradation and conversion processes of organic and inorganic compounds in all tropospheric compartments as well as at phase boundaries. Therefore, OH radical concentrations are an important parameter to describe the oxidation capacity of the tropospheric multiphase system. But, in contrast to gas phase concentrations, direct measurements of the OH radical concentration in tropospheric particles are not available. For this reason aqueous phase OH concentrations reported in the literature solely result from model simulations and therefore depend on the applied model scenario and the quality of the implemented multiphase chemistry mechanisms. Applying the advanced multiphase mechanism CAPRAM 3.0 in its current version in the SPACCIM model framework[8] gives the following OH concentrations in warm clouds and aqueous particles (Table 1). Concentrations in Table 1 were calculated for an urban (polluted), a remote

Prof. Dr. Hartmut Herrmann, Professor of Atmospheric Chemistry, is the head of the Chemistry Department of the Leibniz Institute for Tropospheric Research (see http://www.tropos.de) and a member of both the Faculties of Physics and Chemistry of the University of Leipzig. He finished his Habilitation with Reinhard Zellner in 1998 and then moved from Essen to Leipzig. Previously, he was a scientific assistant at the Institute of Physical Chemistry of the University of Essen (1992–98), a postdoc with Michael Hoffmann at Caltech (1992–93), at Hannover (1991–92) and Göttingen (1990–91) where he obtained both his Diploma (1987) and his Ph.D. (1990) at the Institute of Physical Chemistry. His research aims at a better understanding of tropospheric multiphase chemistry. To this end, his group is engaged in field measurements on aerosols and clouds, laboratory studies of phase transfer, gas and aqueous phase reactions, and, finally, multiphase model development.

Thomas Schaefer is a Ph.D. student in the chemistry department of the Leibniz Institute for Tropospheric Research (IfT). From 2001 to 2007 he studied chemistry at the University of Leipzig. He is currently working on atmospheric aqueous phase reactions.

Peter Bräuer is a Ph.D. student in the chemistry department of the Leibniz Institute for Tropospheric Research (IfT). From 2003 to 2009 he studied meteorology at the University of Leipzig. His research interest lies in the field of atmospheric multiphase chemistry modelling.

Dr. Dirk Hoffmann is a postdoc at the Leibniz Institute for Tropospheric Research (IfT) in Leipzig. He studied chemistry at the University of Leipzig and obtained his Diploma in 2003. Afterwards, he did his PhD (2007) at the IfT. He is currently working on atmospheric aqueous phase reactions.

Dr. Andreas Tilgner studied meteorology at the Faculty of Physics and Earth Science of the University of Leipzig, Germany. Since 2003, he is working at the chemistry department of Leibniz Institute for Tropospheric Research (IfT) in Leipzig, Germany, in the field of tropospheric multiphase chemistry. There, he received his diploma in 2004, worked as a Ph.D. stipend of the DBU (German Federal Environmental Foundation, 2005–2007), received his Ph.D. in April 2009 and is presently working as a research scientist. His research interests and expertise lies mainly in field of tropospheric chemistry modelling with special emphasis on the development of complex multiphase chemical mechanisms and their application in sophisticated tropospheric models.

Table 1. Calculated OH radical concentrations in clouds and deliquescent particles using the CAPRAM 3.0i multiphase mechanism. Mean concentrations are averaged values over three simulation days.

	Urban case: [OH] in mol L^{-1}			Remote case: [OH] in mol L^{-1}			Maritime case: [OH] in mol L^{-1}		
	mean	max	min	mean	max	min	mean	max	min
Cloud droplets	3.5×10^{-15}	1.6×10^{-14}	2.9×10^{-16}	2.2×10^{-14}	6.9×10^{-14}	4.8×10^{-15}	2.0×10^{-12}	5.3×10^{-12}	3.8×10^{-14}
Deliquescent particles	4.4×10^{-13}	1.9×10^{-12}	1.4×10^{-16}	3.0×10^{-12}	8.0×10^{-12}	5.5×10^{-14}	1.0×10^{-13}	3.3×10^{-12}	4.6×10^{-15}

(clean) and a maritime case. The mean concentrations in Table 1 represent averages over three simulation days differing between cloud and deliquescent particle conditions which account for about 14 and 58 h of the 72 h simulation time, respectively. The corresponding concentration time profiles calculated with the latest CAPRAM mechanism can be found in the Supporting Information (Figure S1). More details of the CAPRAM mechanism and the model calculations can be found in Herrmann et al.[2] Wolke et al.[8] and Tilgner and Herrmann.[1] Simulations were carried out for three different atmospheric scenarios, namely remote (continental background case without considerable anthropogenic influence), urban (continental anthropogenic polluted case) and martime (remote ocean case). The three environmental scenarios are characterized by different gas and aqueous phase initial concentrations, different aerosol particle distributions and different emission and deposition rates. The calculated OH concentrations in Table 1 are quite different for the three cases considered and highly variable over the simulation time. Therefore, it is recommended to apply the mean concentration for applications such as lifetime calculations. Highest OH concentrations have been calculated for the maritime and remote case due to less sinks being available.

Sources for OH radicals in the tropospheric aqueous phase are diverse and include processes such as the photolytic decomposition of H_2O_2, Fenton-type reactions between H_2O_2 and transition metal ions (e.g. Fe^{2+}, Cu^{+}), the uptake of OH from the gas phase and the iron complex chemistry.[1,2,9] Atmospheric sinks for OH radicals are also manifold, including reactions with organic and inorganic water soluble compounds of anthropogenic and biogenic origin. Several modeling studies published in the past demonstrate the eminence of reactions with organic compounds as sinks for OH radicals.[1,2,10,11] Therefore, characterizing the kinetics of atmospherically relevant OH radical reactions in aqueous solution is a state-of-the-art science topic and is a prerequisite to describe atmospheric oxidation capacity and chemical conversion processes.

Kinetic measurements of OH radical reactions in aqueous solution are performed in laboratory experiments under controlled conditions by applying different measurement techniques. The most prevalent methods are the pulse radiolysis technique followed by the laser flash photolysis technique. Both techniques use the dissociation of molecules by either light pulses (laser flash photolysis) or accelerated electrons (pulse radiolysis) in order to initiate radical reactions. Other OH radical sources are the continuous lamp exposure of aqueous H_2O_2 solutions as well as the Fenton reaction either in the dark or under irradiation. The main disadvantage of using the Fenton reaction as OH radical source is the introduction of iron in the measurement solution. This makes the chemistry in the reaction solution complex and a careful data evaluation is required to extract the OH radical rate constant. The following sections review the currently available data on OH quantum yields from the H_2O_2 photolysis, the absorption spectra of OH radicals in water, recently published aqueous phase kinetic data relevant for atmospheric chemistry and the most widely applied reference system for kinetic investigations.

2.1. Photochemical Generation from H_2O_2 Photolysis

A widely applied source for OH radicals in aqueous solution is the photolysis of H_2O_2 using either the irradiation by pulsed or continuous-wave (cw) UV lamps or lasers. Therefore, the OH radical quantum yields (Φ_{OH}) for the H_2O_2 photolysis processes have already been investigated since the 1950s. Reported Φ_{OH} in aqueous solution are lower than 2, due to the fast geminate recombination reactions of the OH radicals before they are able to leave the solvent cage.[12,13] The governing molecular processes leading to the observed aqueous phase quantum yields have recently been discussed by Herrmann (2007).[12]

An overview of published Φ_{OH} for H_2O_2 photolysis at different wavelengths is given in Figure 1. As can be seen in Figure 1 some of the data published over the last decades are scattered. However, the majority of the reported quantum

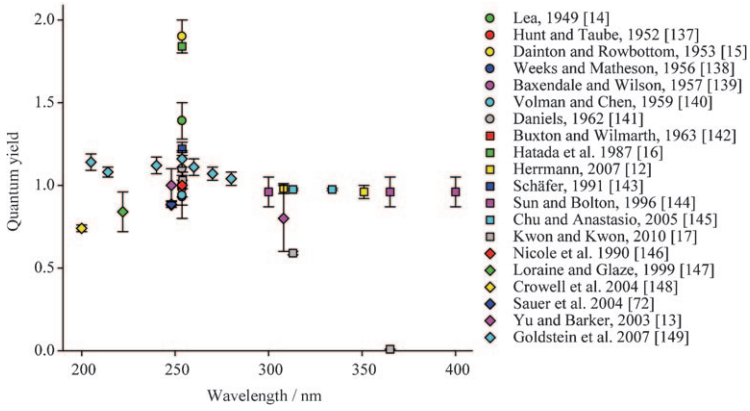

Figure 1. Summary of OH radical quantum yields (Φ_{OH}) for H_2O_2 photolysis in aqueous solution at different photolysis wavelengths. The data are shown in Table S4 in the Supporting Information.

yields in Figure 1 lie within the range of $0.8 \leq \Phi_{OH} \leq 1.2$ for the wavelength range 200 to 400 nm. In most of the studies included in Figure 1 the mercury line ($\lambda = 253.7$ nm) of a Hg lamp has been applied for the H_2O_2 photolysis process. Accordingly, many different values for Φ_{OH} are available in the literature at this specific wavelength. Besides the combination of lamps and filters also monochromatic light sources such as pulsed lasers have been used in some studies. In order to calculate Φ_{OH} changes in the radical concentration in dependency of the number of photons absorbed by H_2O_2 needs to be measured. This implies that the exact determination of quantum yields relies strongly on precise measurements or calculations of both the number of photons entering the reaction solution and the OH radical concentration formed. In order to measure the number of photons different chemical actinometers and different measurement systems such as thermopiles have been applied by the different groups. In particular, chemical actinometers represent very precise, but also rather complicated tools for the measurement of photons. Also the measurement of the OH radical concentration formed in the H_2O_2 photolysis process is not trivial in aqueous solution. In order to calculate the OH radical concentration formed different approaches have been chosen in the past. One commonly used method is the addition of OH scavenger compounds. However, this approach requires both a well-known OH rate constant for the reaction with the scavenger compounds as well as a nonabsorbing scavenger compound at the photolysis wavelength. When scavengers are applied, the effectiveness of the radical conversion into the detectable species depends on the amount and the reactivity of the added scavenger compound. Great care has to taken to characterize a given scavenger system in order to make sure to determine the correct effective quantum yield in question. Additionally, measurement of the H_2O_2 concentration and changes in the gas phase O_2 or CO_2 concentrations have been used to calculate the amount of formed OH. The fact that rather complex measurement systems usually had to be applied instead of direct approaches might be one explanation for the uncertainties observed in the available Φ_{OH} values in Figure 1.

Due to the uncertainties that each measurement system offers the authors suggest to average the existing Φ_{OH} between 240–260 nm as well as the data between 300 and 320 nm. Averaging of quantum yields in a small wavelength range should not be a problem, since the results in Figure 1 do not exhibit a significant wavelength dependence. Only the very high values of Φ_{OH} from Lea,[14] Dainton and Rowbottom[15] and Hatada et al.[16] were not considered for the calculations of the averaged values. Furthermore, values from Kwon and Kwon[17] were not included since their values are apparently too low above 300 nm (Figure 1). The averaged quantum yields are $\Phi_{OH,\ 240-260nm} = 1.02 \pm 0.10$ and $\Phi_{OH,\ 300-320nm} = 0.93 \pm 0.09$.

2.2. The OH Absorption Spectrum in Aqueous Solution

A measurement of the OH radical spectrum in aqueous solution was first published by Thomas and coworkers in 1966.[18]

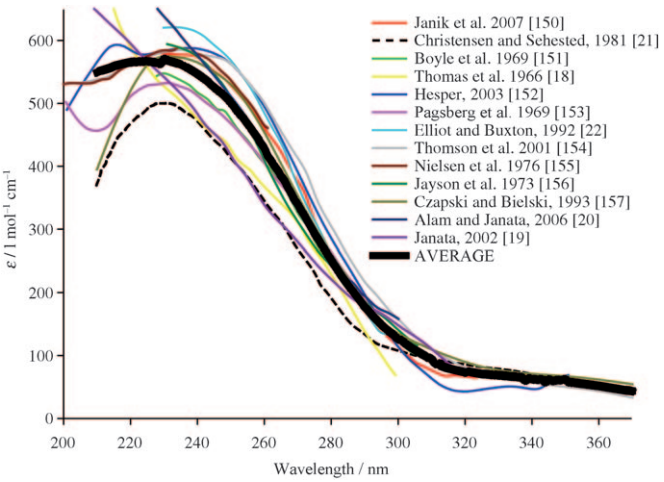

Figure 2. Compilation of digitized OH radical absorption spectra in aqueous solution. The data table of the averaged OH spectra is given in the Supporting Information (Table S1).

Their absorption spectrum (see Figure 2) did not clearly show the typical peak absorption of the OH radical at $\lambda \approx 230$ nm. This peak absorbance around 230 nm was discovered later in different experimental studies. As can be seen in Figure 2, the more recent studies of Janata in 2002[19] or Alam and Janata in 2006[20] do, again, not show this peak absorption at $\lambda =$ 230 nm. The reason for this behavior was explained in the study by Janata.[19] He stated that in his study the hydrogen atom contributes to the measured absorption spectrum below $\lambda < 250$ nm. Additional absorption of H· would certainly explain the missing peak absorbance at $\lambda = 230$ nm. However, the differences in the OH radical spectra reported in Janata, 2002[19] and Alam and Janata, 2006[20] remain unclear, since the later study of Alam cited the study of Janata 2002 as reference for the reported spectra. Since the reasons for this discrepancy could not be clarified both spectra were included in Figure 2.

The absolute decadic absorption coefficients of the OH radical [ε_{10}(OH)] available in the literature are again quite scattered. At the absorbance maximum of the OH radical the differences between the smallest ($\varepsilon_{\lambda=230nm} = 500\ M^{-1}\,cm^{-1}$; Christensen and Sehested[21]) and the highest ($\varepsilon_{\lambda=230nm} = 620\ M^{-1}\,cm^{-1}$; Elliot and Buxton[22]) extinction coefficient published in the literature are 20%. Calculating ε_{OH} based on the absorption spectra of these transient species requires knowledge of the OH radical concentration at the time when the spectra was recorded. Furthermore, the contribution of co-absorbing species needs to be subtracted. Difficulties in the measurement of the OH radical concentration in aqueous solution have been already discussed in the previous chapter. Hence, differences in the extinction coefficient plotted in Figure 2 can be related to both errors in the OH radical concentrations and the subtraction of co-absorbers. In order to account for these differences all absorption spectra shown in Figure 2 have been averaged. The calculated averaged spectrum is shown in Figure 2 and the calculated data points are given in the supplementary material (Table S1). The averaged extinction coefficient at 230 nm corresponds to $\varepsilon_{OH,\lambda=230nm} = 570\ M^{-1}\,cm^{-1}$.

In 2008, Chipman[23] published electronic structure calculations on the influence of water on the absorption spectrum of OH. This paper gives a good overview on the history of OH absorption spectra measurements and reviews the theoretical background of the OH absorption spectra in aqueous solution based on own calculations and available literature.

2.3. OH Kinetics

OH radicals are reactive electrophilic species but, on the other hand, not very selective in nature in comparison to other atmospheric free radicals. The two main reaction mechanisms for OH radicals in aqueous solution are H-abstraction reactions with saturated compounds as well as addition reactions (e.g. to C=C double bonds in unsaturated compounds including aromatics). The probability of electron transfer processes of OH radicals depends strongly on the reduction potentials and the structure of the reactants.

The existing kinetic data set on OH radical reaction in aqueous solution is huge and covers a large variety of chemical reactants. New kinetic studies on OH radical reactions in the last years mainly investigated the reactivity of aromatic compounds, halogenated alkanes, alcohols, carboxylic acids and novel oxygenated solvents in aqueous solution. Based on the existing kinetic data set, structure–activity relationships, computational pathway elucidation models as well as reactivity correlations have been established in the last years describing the reactivity of OH radicals in aqueous solution. Recent developments in this field are summarized and reviewed in a later chapter. Even if it is already possible to describe and predict the kinetics of many OH radical reactions based on measured or estimated data, some questions remains concerning the reactivity, formation and distribution of transient species and stable reaction products. While the degradation schemes of simple aliphatic alcohols, carbonyls and acids are fairly well understood, the reaction paths for aromatic compounds, sugars or other highly functionalized aliphatic reactants are not yet sufficiently understood and require further product characterization. Furthermore, effects of the temperature and the pH are known to influence a reaction rate which is an important aspect for the implementation of kinetic data in atmospheric models. However, the influence of these effects is not routinely measured and hence often not sufficiently parameterized for many of the kinetic data reported in the literature.

Table 2 summarizes the newly measured OH radical kinetic data in aqueous solution being relevant for atmospheric chemistry since 2003. Furthermore, some basic information on the activation energy, the pre-exponential factor of the Arrhenius equation, the measurement technique, the experimental conditions and the applied reference system is given.

The coding in Table 2 (see the column captioned Comments and the legend to Table 2) provides additional information whether a first-time determination (index 1) of a rate constant or a new measurement of an already investigated and reviewed reaction (index 2) is considered. In case of a remeasurement it is marked in Table 2, if more than one literature value exists by an asterisk (*) The coding of Table 2 also provides information if a newly measured rate constant agrees with the averaged value of the already published rate constants within a factor of two (indicated by A) or not (indicated by B). As can be seen from the data of Table 2, recent OH kinetic data of interest for atmospheric chemistry have been obtained for aliphatic alcohols, oxygenated compounds, halogenated compounds, amines, aromatics and a couple of inorganic compounds.

Aliphatic alcohols

A number of rate constants have been obtained from our laboratory[24] for reactions of OH with diols, including temperature dependence and a number of sugars of interest for atmospheric particle chemistry. Moreover, Arrhenius parameters are now available for these reactions, often for the first time. In addition, a number of reactions of OH with the most simple C_1–C_4 alcohols have also been investigated again with results not differing much from the already available data as summarized earlier,[3,7] as a new experimental setup was tested by Alam and coworkers.[25] In most cases, competition kinetic methods were applied mostly with thiocyanate as the reference system and sometimes using the propanols as reference compounds. All data, with the exceptions of 1,2-butanediol and levoglucosan, in this substance class are no first measurement but in agreement with the former determinations and hence classified as 2A in the Comments column of Table 2.

Oxygenated Compounds

A number of compounds of interest because of their industrial use have been investigated in the MOST EC project in studies by Gligorovski et al.,[26] Moise et al.[27] and Monod et al.[28] The reactivity of substituted ethers was also studied by Mezyk et al.[29] Within this compound class, a number of temperature dependences are available now. Finally, in the studies of Bardouki et al.[30] and Zhu et al.,[31] aqueous phase reaction data of interest for the atmospheric multiphase oxidation of dimethyl sulfide (DMS) are available. In this substance group there are eleven new determinations and seventeen remeasurements, most of which are in reasonable agreement with the formerly available measurements (class 2A) with the exception of the measurement of the reaction of OH with methylglyoxal, indexed as 2B and to be discussed in the following (see Table 3).

The differences in the results of both studies using two different experimental techniques are slightly higher than the defined threshold value of two herein. The different rate constants obtained have been discussed by Monod et al.,[28] but there are no clear answers what is causing the difference of a factor of two. The reference rate constants used in both studies are in agreement with the literature values for these reactions. Possibly, in one of the available studies there might have been fractions of oligomerised methylglyoxal present in the measurement solutions. To clarify the situation for this reaction of large interest for atmospheric chemistry, another remeasurement of this reaction is currently under progress in our laboratory.

Table 2. Compilation of newly measured aqueous phase OH radical kinetic data relevant for atmospheric chemistry. Coding and abbreviations are explained in the text or below the Table.

Reactant	Technique	pH	k_{2nd} [$M^{-1}s^{-1}$]	Comments	A [$M^{-1}s^{-1}$]	E_A [kJ mol^{-1}]	Measuring technique	$k_{ref,298K}$ [$M^{-1}s^{-1}$]	Ref.
Aliphatic alcohols									
1,2-ethanediol	LFP/H_2O_2	~6	$(1.7\pm0.03)\times10^9$	2, A*, □,○	$(9.0\pm0.3)\times10^{10}$	9.9 ± 2.0	C.K./SCN^-	1.24×10^{10}	[24]
1,2-propanediol	LFP/H_2O_2	~6	$(1.7\pm0.3)\times10^9$	2, A, □,○	$(1.9\pm0.2)\times10^{11}$	11.5 ± 8.6	C.K./SCN^-	1.24×10^{10}	[24]
1,3-propanediol	LFP/H_2O_2	~6	$(2.7\pm0.2)\times10^9$	2, A, □,○	$(2.5\pm0.2)\times10^{11}$	11.4 ± 6.3	C.K./SCN^-	1.24×10^{10}	[24]
1,2,3-propanetriol	LFP/H_2O_2	~6	$(2.3\pm0.4)\times10^9$	2, A*, □,○	$(2.8\pm0.2)\times10^{11}$	12.3 ± 4.0	C.K./SCN^-	1.24×10^{10}	[24]
1,2-butanediol	LFP/H_2O_2	~6	$(1.7\pm0.03)\times10^9$	1	$(5.2\pm0.5)\times10^{11}$	13.3 ± 7.0	C.K./SCN^-	1.24×10^{10}	[24]
1,4-butanediol	LFP/H_2O_2	~6	$(3.5\pm0.1)\times10^9$	2, A, □,○	$(2.0\pm0.05)\times10^{11}$	10.0 ± 1.8	C.K./SCN^-	1.24×10^{10}	[24]
1,5-pentanediol	LFP/H_2O_2	~6	$(4.4\pm0.7)\times10^9$	2, A, □,○	$(3.1\pm0.1)\cdot10^{11}$	10.6 ± 2.8	C.K./SCN^-	1.24×10^{10}	[24]
erythritol	LFP/H_2O_2	~6	$(1.9\pm0.2)\times10^9$	2, A, □,○	$(1.3\pm0.04)\times10^{12}$	16.2 ± 1.8	C.K./SCN^-	1.24×10^{10}	[24]
arabitol	LFP/H_2O_2	~6	$(1.6\pm0.2)\times10^9$	2, A, □,○	$(2.5\pm0.1)\times10^{10}$	6.6 ± 3.5	C.K./SCN^-	1.24×10^{10}	[24]
mannitol	LFP/H_2O_2	~6	$(1.6\pm0.3)\times10^9$	2, A*, □,○	$(1.8\pm0.1)\times10^{10}$	6.1 ± 1.8	C.K./SCN^-	1.24×10^{10}	[24]
levoglucosan	LFP/H_2O_2	~6	$(2.4\pm0.3)\times10^9$	1	$(8.7\pm0.4)\times10^{10}$	9.0 ± 2.9	C.K./SCN^-	1.24×10^{10}	[110]
methanol	CFS/H_2O_2	8.7	$(7.6\pm0.7)\times10^8$	2, A*, □,○,●	–	–	C.K./PNDA	1.25×10^{10}	[49]
	PR	<7	9.0×10^8	2, A*, □,○,●	–	–	direct	–	[25]
ethanol	SPR/PhotoFenton	2	$(2.1\pm0.2)\times10^9$	2, A*, □,○,●	3.2×10^{10}	6.9	C.K./MeOH	9.8×10^8	[28]
	CFS/H_2O_2	8.7	$(1.4\pm0.6)\times10^9$	2, A*, □,○,●	–	–	C.K./PNDA	1.25×10^{10}	[49]
	PR	<7	2.2×10^9	2, A*, □,○,●	–	–	direct	–	[25]
1-propanol	SPR/Fenton	2	$(2.7\pm0.7)\times10^9$	2, A*, □,○,●	4.4×10^{10}	6.5	C.K./2-PrOH	1.9×10^9	[28]
2-propanol	SPR/PhotoFenton	2	$(1.9\pm0.2)\times10^9$	2, A*, □,○,●	–	–	C.K./1-PrOH	2.8×10^9	[28]
	PR	<7	2.0×10^9	2, A*, □,○,●	–	–	direct	–	[25]
1-butanol	SPR/PhotoFenton	2	$(4.2\pm0.4)\times10^9$	2, A*, □,○,●	–	–	C.K./2-PrOH	1.9×10^9	[28]
t-butanol	SPR/PhotoFenton	2	$(7.0\pm2.0)\times10^8$	2, A*, □,○,●	–	–	C.K./2-PrOH	1.9×10^9	[28]
	PR	<7	6.2×10^8	2, A*, □,○,●	–	–	direct	–	[25]
Oxygenated compounds									
DVE-3	LFP/TeflonWG	6–7	$(1.6\pm0.2)\times10^{10}$	1	$(2.3\pm0.1)\times10^{13}$	18.1 ± 2.9	C.K./SCN^-	1.24×10^{10}	[26]
methacrolein	LFP/TeflonWG	6–7	$(1.4\pm0.3)\times10^{10}$	2, A, ●	$(3.0\pm0.1)\times10^{13}$	19.0 ± 1.4	C.K./SCN^-	1.24×10^{10}	[26]
methylglyoxal	SPR/PhotoFenton	2	$(5.3\pm0.4)\times10^8$	2, B, ●	2.0×10^{10}	9.1	C.K./2-PrOH	1.9×10^9	[28]
2-butanone	SPR/PhotoFenton	2	$(8.1\pm1.8)\times10^8$	2, A*, □,○,●	2.4×10^{11}	13.3	C.K./2-PrOH	1.9×10^9	[28]
acetone	PR	7	$(9.5\pm0.2)\times10^7$	2, A*, □,○,●	–	–	C.K./SCN^-	1.10×10^{10}	[111]
	LFP/TWG	6–7	$(1.8\pm0.4)\times10^8$	2, A*, □,○,●	–	–	C.K./SCN^-	1.24×10^{10}	[26]
	UV/H_2O_2	2	$(1.2\pm0.6)\times10^8$	2, A*, □,○,●	1.6×10^{10}	11.6	C.K./MeOH	9.8×10^8	[28]
methylisobutylketone	LFP/TWG	6–7	$(4.6\pm1.6)\times10^9$	2, A,●	$(1.0\pm0.1)\times10^{12}$	13 ± 5	C.K./SCN^-	1.24×10^{10}	[26]
	UV/H_2O_2	2	$(2.1\pm0.5)\times10^9$	2, A,●	1.3×10^{11}	10.0	C.K./MeOH	9.8×10^8	[28]
n-methylpyrrolidone	LFP/TWG	6–7	$(4.9\pm2.3)\times10^9$	2, A*, □,○,●	$(1.8\pm0.2)\times10^{11}$	8.8 ± 6.7	C.K./SCN^-	$1.24\cdot10^{10}$	[26]
acetonylacetone	TWG	n.r.	$(1.8\pm0.9)\times10^9$	2, A*, ●	–	–	C.K./SCN^-	1.29×10^{10}	[27]
isobutyraldehyde	TWG	n.r.	$(2.9\pm1.5)\times10^9$	2, A, ●	–	–	C.K./SCN^-	1.29×10^{10}	[27]
di(ethylene glycol) vinyl ether	TWG	n.r.	$(4.2\pm2.1)\times10^{10}$	1	–	–	C.K./SCN^-	1.29×10^{10}	[27]
di(ethylene glycol) divinyl ether	TWG	n.r.	$(2.3\pm2.1)\times10^{10}$	1	–	–	C.K./SCN^-	1.29×10^{10}	[27]
tri(ethylene glycol) divinyl ether	TWG	n.r.	$(4.8\pm2.4)\times10^{10}$	1	–	–	C.K./SCN^-	1.29×10^{10}	[27]
2,3-dimethyl-1,3-butadiene	TWG	n.r.	$(3.1\pm1.6)\times10^{10}$	1	–	–	C.K./SCN^-	1.29×10^{10}	[27]
hydroxybutyl vinyl ether	TWG	n.r.	$(1.9\pm0.9)\times10^9$	1	–	–	C.K./SCN^-	1.29×10^{10}	[27]
t-butylethylether	SPR/PhotoFenton	2	$(1.5\pm1.7)\times10^9$	2, A,○	$1.2\cdot10^{10}$	4.8	C.K./2-PrOH	1.9×10^9	[28]

Table 2. (Continued)

Reactant	Technique	pH	k_{2nd} [$M^{-1}s^{-1}$]	Comments	A [$M^{-1}s^{-1}$]	E_A [kJ mol^{-1}]	Measuring technique	$k_{ref,298K}$ [$M^{-1}s^{-1}$]	Ref.
n-butylacetate	SPR/PhotoFenton	2	$(1.8\pm0.4)\times10^9$	1	5.3×10^{10}	8.3	C.K./2-PrOH	1.9×10^9	[28]
t-butyl formate	PR	7	$(5.2\pm0.1)\times10^8$	2, A,●	–	–	C.K./SCN^-	1.05×10^{10}	[112]
2-methoxy-2-methyl-propanal	PR	7	$(4.0\pm0.3)\times10^9$	1	–	–	C.K./SCN^-	1.05×10^{10}	[29]
2-methoxy-2-methyl-propanol	PR	7	$(8.0\pm0.5)\times10^8$	1	–	–	C.K./SCN^-	1.05×10^{10}	[29]
2-methoxy-2-methyl-propanoic acid	PR	7	$(7.7\pm0.5)\times10^8$	1	–	–	C.K./SCN^-	1.05×10^{10}	[29]
dimethylsulfoxide (DMSO)	LFP	5–6	$(6.3\pm0.5)\times10^9$	2, A*, □,○	4.7×10^{11}	10.6	C.K./SCN^-	1.2×10^{10}	[31]
	UV/H_2O_2	6	4.5×10^9	2, A*, □,○	–	–	Product analysis	–	[30]
dimethylsulfone ($DMSO_2$)	LFP	5–6	$\leq(1.7\pm0.2)\times10^7$	2, A, ○	5.1×10^9	14.1	C.K./SCN^-	1.2×10^{10}	[31]
methanesulfonate (MS)	LFP	5–6	$(1.2\pm0.2)\times10^7$	2, A, ○	8.8×10^{10}	21.9	C.K./SCN^-	1.2×10^{10}	[31]
methanesulfinate (MSI)	UV/H_2O_2	6	1.2×10^{10}	1	–	–	Product analysis	–	[30]
Carboxylic acids									
malic acid	LFP/TeflonWG	1	$(3.6\pm1.6)\times10^8$	2, A*, □,○,●	$(7.9\pm0.8)\times10^{10}$	13 ± 7	C.K./SCN^-	1.24×10^{10}	[26]
maleate (mono-anion)	LFP/TeflonWG	4.3	$(9.7\pm2.5)\times10^9$	1	$(2.9\pm0.4)\times10^{11}$	14 ± 10	C.K./SCN^-	1.24×10^{10}	[26]
maleate (di-anion)	LFP/TeflonWG	9	$(8.5\pm1.1)\times10^8$	2, A*, ○,●	$(1.2\pm0.2)\times10^{11}$	12 ± 10	C.K./SCN^-	1.24×10^{10}	[26]
oxalate (mono-anion)	PR	2.5–3.5	$(5.5\pm0.5)\times10^7$	2, B, ○,●	–	–	direct/fitted	–	[32]
mesoxalic acid	LFP/TeflonWG	1	$(1.8\pm0.3)\times10^8$	1	$(3.8\pm0.8)\times10^{10}$	13.2 ± 12.7	C.K./SCN^-	1.24×10^{10}	[26]
mesoxalate (di-anion)	LFP/TeflonWG	9	$(2.2\pm0.6)\times10^9$	2, B	–	–	C.K./SCN^-	1.24×10^{10}	[26]
lactic acid	PR	1	$(5.2\pm0.4)\times10^8$	2, A*, □,○	2.3×10^{10}	9.3 ± 0.5	C.K./SCN^-	1.05×10^{10}	[33]
lactate	PR	6.1	$(7.8\pm0.5)\times10^8$	2, A*, □,○	6.1×10^{10}	10.8 ± 0.3	C.K./SCN^-	1.05×10^{10}	[33]
Halogenated alkanes									
2-Fluoroethanol	LFP/H_2O_2	5.5–6.5	$(5.4\pm1.8)\times10^8$	1	$(5.7\pm0.8)\times10^{11}$	17 ± 10	C.K./SCN^-	1.24×10^{10}	[39]
2,2-Difluoroethanol	LFP/H_2O_2	5.5–6.5	$(2.8\pm0.7)\times10^8$	1	$(4.5\pm0.5)\times10^9$	7 ± 7	C.K./SCN^-	1.24×10^{10}	[39]
2,2,2-Trifluoroethanol	LFP/H_2O_2	5.5–6.5	$(8.5\pm2.5)\times10^7$	2, B, ○	$(2.0\pm0.1)\times10^{11}$	20 ± 7	C.K./SCN^-	1.24×10^{10}	[39]
2-Chloroethanol	LFP/H_2O_2	5.5–6.5	$(8.6\pm0.7)\times10^8$	2, A, □,○	$(3.0\pm0.2)\times10^{10}$	9 ± 4	C.K./SCN^-	1.24×10^{10}	[39]
2,2-Dichloroethanol	LFP/H_2O_2	5.5–6.5	$(3.9\pm0.8)\times10^8$	1	$(2.1\pm0.2)\times10^{10}$	10 ± 4	C.K./SCN^-	1.24×10^{10}	[39]
2,2,2-Trichloroethanol	LFP/H_2O_2	5.5–6.5	$(2.4\pm1.1)\times10^8$	2, B,●	$(1.6\pm0.1)\times10^{10}$	10 ± 5	C.K./SCN^-	1.24×10^{10}	[39]
chloronitromethan	PR	~7	$(1.9\pm0.3)\cdot10^8$	1	–	–	C.K./SCN^-	1.05×10^{10}	[40]
dichloronitromethan	PR	~7	$(5.1\pm0.8)\times10^8$	1	–	–	C.K./SCN^-	1.05×10^{10}	[40]
dibromonitromethan	PR	~7	$(4.8\pm1.0)\times10^8$	1	–	–	C.K./SCN^-	1.05×10^{10}	[40]
tribromonitromethan	PR	~7	$(3.3\pm0.7)\times10^8$	1	–	–	C.K./SCN^-	1.05×10^{10}	[40]
bromochloronitromethan	PR	~7	$(4.2\pm1.1)\times10^8$	1	–	–	C.K./SCN^-	1.05×10^{10}	[40]
bromodichloronitromethan	PR	~7	$(1.0\pm0.2)\times10^8$	1	–	–	C.K./SCN^-	1.05×10^{10}	[40]
dibromochloronitromethan	PR	~7	$(1.8\pm0.3)\times10^8$	1	–	–	C.K./SCN^-	1.05×10^{10}	[40]
tribromomethan	PR	~7	$(1.5\pm0.05)\times10^8$	1	–	–	C.K./SCN^-	1.05×10^{10}	[40]
bromodichloromethan	PR	~7	$(7.1\pm0.3)\times10^7$	1	–	–	C.K./SCN^-	1.05×10^{10}	[40]
chlorodibromomethan	PR	~7	$(8.3\pm0.3)\times10^7$	1	–	–	C.K./SCN^-	1.05×10^{10}	[40]
monochloroethane	PR	n.r.	5.5×10^8	1	–	–	C.K./SCN^-	1.40×10^{10}	[41]
1,1-dichloroethane	PR	n.r.	1.3×10^8	1	–	–	C.K./SCN^-	1.40×10^{10}	[41]
1,2-dichloroethane	PR	n.r.	2.2×10^8	1	–	–	C.K./SCN^-	1.40×10^{10}	[41]
1,1,1-trichloroethane	PR	n.r.	$<0.05\times10^8$	1	–	–	C.K./SCN^-	1.40×10^{10}	[41]
1,1,2-trichloroethane	PR	n.r.	3.0×10^8	1	–	–	C.K./SCN^-	1.40×10^{10}	[41]
1,1,1,2-tetrachloroethane	PR	n.r.	0.1×10^8	1	–	–	C.K./SCN^-	1.40×10^{10}	[41]
1,1,2,2-tetrachloroethane	PR	n.r.	2.5×10^8	1	–	–	C.K./SCN^-	1.40×10^{10}	[41]
pentachloroethane	PR	n.r.	$<0.05\times10^8$	1	–	–	C.K./SCN^-	1.40×10^{10}	[41]
Amines									
methylethylnitrosamine	PR	~7	$(5.0\pm0.2)\times10^8$	1	–	–	C.K./SCN^-	1.05×10^{10}	[47]
diethylnitrosamine	PR	~7	$(7.0\pm0.3)\times10^8$	1	–	–	C.K./SCN^-	1.05×10^{10}	[47]
dimethylnitramine	PR	~7	$(5.4\pm0.2)\times10^8$	1	–	–	C.K./SCN^-	1.05×10^{10}	[47]
methylethylnitramine	PR	~7	$(7.6\pm0.4)\times10^8$	1	–	–	C.K./SCN^-	1.05×10^{10}	[47]
diethylnitramine	PR	~7	$(8.7\pm0.5)\times10^8$	1	–	–	C.K./SCN^-	1.05×10^{10}	[47]
Aromatic compounds									
phenol	SPR/PhotoFenton	2	$(1.9\pm0.2)\cdot10^9$	2, B, □,○	–	–	C.K./2-PrOH	1.9×10^9	[28]
chlorobenzene	PR	10	6.2×10^9	2, A, ○,□	–	–	direct/PBK	–	[48]
2-chlorbenzoate ion	PR	10	5.8×10^9	2, A, ○,□	–	–	direct/PBK	–	[48]
3-chlorbenzoate ion	PR	10	5.4×10^9	2, A, ○,□	–	–	direct/PBK	–	[48]

Table 2. (Continued)

Reactant	Technique	pH	k_{2nd} [$M^{-1}s^{-1}$]	Comments	A [$M^{-1}s^{-1}$]	E_A [kJ mol^{-1}]	Measuring technique	$k_{ref,298K}$ [$M^{-1}s^{-1}$]	Ref.
4-chlorbenzoate ion	PR	10	4.5×10^{9}	2, A, ○,□	–	–	direct/PBK	–	[48]
benzoate	CFS/H_2O_2	8.7	$(2.5\pm1.6)\times10^{9}$	2, B*, ○,□	–	–	C.K./PNDA	1.25×10^{10}	[49]
2-hydroxybenzoate	CFS/H_2O_2	8.7	$(3.9\pm1.2)\times10^{9}$	2, B*, ○	–	–	C.K./PNDA	1.25×10^{10}	[49]
3-hydroxybenzoate	CFS/H_2O_2	8.7	$(2.5\pm1.6)\times10^{9}$	1	–	–	C.K./PNDA	1.25×10^{10}	[49]
4-hydroxybenzoate	CFS/H_2O_2	8.7	$(2.3\pm0.4)\times10^{9}$	2, B*, ○,□	–	–	C.K./PNDA	1.25×10^{10}	[49]
4-chloro-3,5-dinitrobenzoic acid	UV/H_2O_2	2.5	$(3.3\pm0.2)\times10^{8}$	1	–	–	C.K.	–	[50]
1-chloro-2,4-dinitrobenzene	UV/H_2O_2	2.5	$(8.2\pm0.5)\times10^{8}$	1	–	–	C.K./CDNBA	3.3×10^{8}	[50]
1,3-dinitrobenzene	UV/H_2O_2	2.5	$(1.1\pm0.5)\times10^{9}$	1	–	–	C.K./CDNB	8.2×10^{8}	[50]
2,4-dinitrophenol	UV/H_2O_2	2.5	$(2.3\pm0.4)\times10^{9}$	1	–	–	C.K./CDNBA	3.3×10^{8}	[50]
nitrobenzene	UV/H_2O_2	2.5	$(4.2\pm0.4)\times10^{9}$	2, A*, ○,□	–	–	C.K./CDNBA	3.3×10^{8}	[50]
	PR	7	$(3.0\pm0.2)\times10^{9}$	2, A*, ○,□	–	–	direct/PBK	–	[51]
3-nitrophenol	UV/H_2O_2	2.5	$(5.0\pm0.4)\times10^{9}$	1	–	–	C.K./CDNB	8.2×10^{8}	[50]
2-nitrophenol	UV/H_2O_2	2.5	$(5.9\pm0.7)\times10^{9}$	1	–	–	C.K./PNP	6.2×10^{9}	[50]
4-nitrophenol	UV/H_2O_2	2.5	$(6.2\pm0.6)\times10^{9}$	2, A*, ○,□	–	–	C.K./CDNB	8.2×10^{8}	[50]
3-nitrotoluene	UV/H_2O_2	2.5	$(8.6\pm0.5)\cdot10^{9}$	1	–	–	C.K./NBE	4.2×10^{9}	[50]
4-nitrotoluene	UV/H_2O_2	2.5	$(8.2\pm0.5)\times10^{9}$	1	–	–	C.K./NBE	4.2×10^{9}	[50]
2,4,6-trinitrotoluene	PR	n.r.	$(7.4\pm0.8)\times10^{8}$	1	–	–	C.K./SCN^-	6.6×10^{9}	[52]
2,4-dinitrotoluene	PR	n.r.	$(9.0\pm0.8)\times10^{8}$	1	-	-	C.K./SCN^-	6.6×10^{9}	[52]
	PR	7	$(1.2\pm0.02)\times10^{9}$	1	–	–	direct/PBK	–	[51]
	UV/H_2O_2	7	$(1.4\pm0.1)\times10^{9}$	1	–	–	C.K./Nitroben-zene	6.9×10^{9}	[51]
2,6-dinitrotoluene	PR	7	$(7.8\pm0.1)\cdot10^{8}$	1	–	–	direct/PBK	–	[51]
	UV/H_2O_2	7	$(1.5\pm0.1)\cdot10^{9}$	1	–	–	C.K./molinate	3.9×10^{9}	[51]
benzaldehyde	PR	n.r.	2.6×10^{9}	2, A, ○,□	–	–	direct/PBK	–	[53]
3-hydroxybenzaldehyde	PR	n.r.	7.7×10^{9}	1	–	–	direct/PBK	–	[53]
4-hydroxybenzaldehyde	PR	n.r.	1.2×10^{10}	1	–	–	direct/PBK	–	[53]
3-methoxybenzaldehyde	PR	n.r.	8.0×10^{9}	1	–	–	direct/PBK	–	[53]
4-methoxybenzaldehyde	PR	n.r.	1.1×10^{10}	1	–	–	direct/PBK	–	[53]
3-chlorobenzaldehyde	PR	n.r.	3.1×10^{9}	1	–	–	direct/PBK	–	[53]
4-chlorobenzaldehyde	PR	n.r.	2.8×10^{9}	1	–	–	direct/PBK	–	[53]
3-nitrobenzaldehyde	PR	n.r.	3.0×10^{9}	1	–	–	direct/PBK	–	[53]
4-nitrobenzaldehyde	PR	n.r.	3.0×10^{9}	1	–	–	direct/PBK	–	[53]
Inorganic compounds									
iodine anion	PR	10	1.6×10^{10}	2, A*, ○,□	–	–	direct/fitted	–	[57]
thiocyanate	PR	6–7	$(1.4\pm0.1)\times10^{10}$	2, A*, ○,□	–	–	direct/PBK	–	[58]
hydrogen peroxide	LFP	0–4	$(4.2\pm0.2)\times10^{7}$	2, A*, ○,□	–	–	calculated	–	[113]
bromide	CFS/H_2O_2	8.7	$(4.2\pm1.6)\times10^{9}$	2, B, ○,□	–	–	C.K./PNDA	1.25×10^{10}	[49]
chloride	CFS/H_2O_2	8.7	$(2.8\pm1.7)\times10^{9}$	2, A*, ○,□	–	–	C.K./PNDA	1.25×10^{10}	[49]
carbonate	CFS/H_2O_2	8.7	$(3.5\pm0.4)\times10^{8}$	2, A*, ○,□	–	–	C.K./PNDA	1.25×10^{10}	[49]
bicarbonate	CFS/H_2O_2	8.7	$(1.9\pm0.3)\times10^{7}$	2, A*, ○,□	–	–	C.K./PNDA	1.25×10^{10}	[49]
thiosulphate	CFS/H_2O_2	8.7	$(3.7\pm1.3)\times10^{9}$	2, A*, ○,□	–	–	C.K./PNDA	1.25×10^{10}	[49]
sulfite	CFS/H_2O_2	8.7	$(3.6\pm1.2)\times10^{9}$	2, A*, ○,□	–	–	C.K./PNDA	1.25×10^{10}	[49]

PR = Pulse radiolysis; LFP = Laser flash photolysis; CFS = Continuous-flow system; SPR = Static photoreactor; TWG = Teflon waveguide; UV = UV-lamp photolysis; PBK = Product build-up kinetics; C.K. = Competition kinetics; PNDA = *p*-nitrosodimethylaniline; NBE = nitrobenzene; CDNB = 1-chloro-2,4-dinitrobenzene; CDNBA = 4-chloro-3,5-dinitrobenzoic acid; PNP = 4-nitrophenol; ● Herrmann[7]; ○ NIST[6]; □ Buxton et al.[3]

Table 3. Summary of the available kinetic data measured for the reaction between OH and methylglyoxal at $T = 298$ K in aqueous solution.

Technique	pH	k_{2nd} $M^{-1}s^{-1}$	Measuring technique	$k_{ref,298K}$ $M^{-1}s^{-1}$	Reference
SPR/PhotoFenton	2	$(5.3\pm0.4)\times10^{8}$	C.K./2-PrOH	1.9×10^{9}	[28]
LFP/H_2O_2	4.5	$(1.1\pm0.2)\times10^{9}$	C.K./SCN^-	1.24×10^{10}	[36]
Averaged value		8.2×10^{8}			

Carboxylic Acids/Dicarboxylic Acids

A set of rate constant for the dicarboxylic acids malic, maleic, and mesoxalic and their respective mono- and dianions is available from Gligorovski et al.[26] including the temperature dependences. Ershov et al.[32] and Martin et al.[33] determined the rate constants for the reactions of OH with oxalic and lactic acid, respectively, at room temperature. Out of the eight new rate constants available, two are new for the reactions of maleate monoanion and mesoxalic acid while four more rate constants are not strongly different from the available literature data (2A). However, there

Table 4. Summary of the available kinetic data measured for the reaction between OH and oxalic acid at $T = 298$ K in aqueous solution.

Technique	pH	k_{2nd} [$M^{-1}s^{-1}$]	Measuring technique	$k_{ref,298K}$ [$M^{-1}s^{-1}$]	Ref.
PR	2.5–3.5	$(5.5\pm0.5)\times10^7$			[32]
PR	3.0	$(3.2\pm0.1)\times10^7$	C.K./SCN^-		[34]
		3.5×10^7			[35]
LFP/H_2O_2	3.0	$(1.9\pm0.6)\times10^8$	C.K./SCN^-	1.24×10^{10}	[36]

are discrepancies for the available rate constants for oxalate monoanion (Table 4).

The rate constant measured by Ershov et al.[32] for the oxalate mono-anion fit well in to the previously available data by Getoff et al.[34] and Draganic et al.[35] and appears to confirm the slower rate constants from the earlier studies. However, the older values and the more recent one by Ershov is significantly slower than the value reported by Ervens et al.[36] measured at the same pH. The reason for this dicrepancy is unclear and needs clarification because of the atmospheric importance of this reaction.

As can be seen from Table 5, there is also no consistency in the kinetic data for the reaction of OH with mesoxalic acid in its three forms. Apparently, there is a difference in the measured rate constants at pH 9 for the mesoxalate dianion which amounts to a factor of twenty. These differences cannot be explained by the usage of slightly different reference rate constants only. However, mesoxalic acid is absorbing light at the photolysis wavelength of 248 nm used in the study of Gligorovski and co-workers.[26] Therefore, photolysis processes of mesoxalic acid and mesoxalate dianion might have an influence on the reactant concentrations and the chemistry during the measurements in their study. The same is also valid for the measurements of Gligorovski[26] at pH 1. Furthermore, the pH values in both the studies of Gligorovski et al.[26] as well as Schuchmann et al.[37] at pH 1 and pH 3, are quite close to the two pK_A values ($pK_{A1} = 1.82$ and $pK_{A2} = 3.52$)[38] of mesoxalic acid. Consequently, even small changes in the pH during the measurement will affect the dissociation grade and subsequently the reactivity. Since there is no consistent data set available no recommendation can be given by the authors at this point.

Table 5. Summary of the available kinetic data measured for the reaction between OH and mesoxalic acid at different pH ($T = 298$ K) in aqueous solution.

Technique	pH	k_{2nd} [$M^{-1}s^{-1}$]	Measuring technique	$k_{ref,298K}$ [$M^{-1}s^{-1}$]	Ref.
		Mesoxalic acid			
LFP/Teflon	1	$(1.8\pm0.3)\times10^8$	C.K./SCN^-	1.24×10^{10}	[26]
		Mesoxalate (mono-anion)			
PR	3	5.7×10^7	C.K./SCN^-	1.1×10^{10}	[37]
		Mesoxalate (di-anion)			
LFP/TeflonWG	9	$(2.2\pm0.6)\times10^9$	C.K./SCN^-	1.24×10^{10}	[26]
PR	9	1.0×10^8	C.K./SCN^-	1.1×10^{10}	[37]

Halogenated Alkanes

Morozov et al.[39] studied the reaction of OH with a number of halogenated ethanols as a function of temperature. Mezyk et al.[40] present kinetic investigations of halogen-substituted methanes in water, whereas halogen-substituted ethanes have been investigated by Milosavljevic et al.[41] Strikingly, as long as the compounds carry an abstractable H atom, the room-temperature rate constants are in the range of 1×10^8 $M^{-1}s^{-1}$. In this substance group, there are 21 new determinations and only three redeterminations, in two of which (2,2,2-trifluoroethanol and 2,2,2-trichloroethanol) differences to former studies occur as can be seen from Table 6.

Table 6. Summary of the available kinetic data measured for OH radical reactions with 2,2,2-trifluoroethanol and 2,2,2-trichloroethanol at $T = 298$ K in aqueous solution.

Technique	pH	k_{2nd} [$M^{-1}s^{-1}$]	Measuring technique	$k_{ref,298K}$ [$M^{-1}s^{-1}$]	Ref.
		2,2,2-trifluoroethanol			
LFP/H_2O_2	5.5–6.5	$(8.5\pm2.5)\times10^7$	C.K./SCN^-	1.24×10^{10}	[39]
Fenton	<2	2.3×10^8	C.K./Fe^{2+}	4.3×10^8	[42]
PR	6.6	$(7.5\pm1.5)\times10^7$	C.K./SCN^-	1.1×10^{10}	[43]
PR	11.6	1.5×10^9	C.K./SCN^-	1.1×10^{10}	[43]
Averaged value		8×10^7			
		2,2,2-trichloroethanol			
LFP/H_2O_2	5.5–6.5	$(2.4\pm1.1)\times10^8$	C.K./SCN^-	1.24×10^{10}	[39]
Fenton	<2	4.2×10^8	C.K./Fe^{2+}	4.3×10^8	[42]
PR	6.6	$(1.5\pm0.3)\times10^8$	C.K./SCN^-	1.1×10^{10}	[43]
PR	11.6	1.9×10^9	C.K./SCN^-	1.1×10^{10}	[43]
Averaged value		1.95×10^8			

The rate constants for 2,2,2-trifluoroethanol and 2,2,2-trichloroethanol reported in Morozov et al.[39] are smaller than the available data from Walling et al.[42] Measurements of Walling et al.[42] were done in very acidic solution using the reaction between OH and Fe^{2+} as reference reaction, which is a quite complex reference system. Furthermore, the applied reference rate constant of Walling et al.[42] is the fastest available for this reaction in the literature. In both cases the lower reactivities measured by Morozov et al.[39] are further supported by the measurements of Alfassi et al.[43] in 1996 at pH 6.6. Alfassi and co-authors[43] also stated that these reactivities are practically identical to the gas-phase values. Therefore, it is suggested to exclude the data from Walling et al.[42] and to average only the data from Alfassi et al.[43] and Morozov et al.[39] at pH ~ 6. The higher rate constants for both compounds at pH 11.6 can be explained by the dissociation of the two compounds at this pH.

Amines

Amines are currently heavily discussed in atmospheric chemistry due to their abundance in marine[44,45] and small, newly formed[46] particles. Furthermore, the reactions of OH with some derivatives such as nitrosamines and nitramines have been newly investigated by Mezyk et al.[47]

Aromatics

A number of new rate constants is available for mostly deactivated aromatic benzene, phenol and benzoic acid derivatives from the studies of Monod et al.,[28] Zona et al.,[48] Kwon et al.,[49] Einschlag et al.,[50] Elovitz et al.,[51] Makarov et al.,[52] Elovitz et al.,[51] and Geeta et al.[53] All reported data do refer to room temperature rate constants only with 23 new determinations and 12 remeasurements, and for four major differences in the rate constants are observed (Table 7).

Kwon et al.[49] introduced a continuous-flow system for the measurement of aqueous-phase OH radical rate constants using competition kinetic method. These authors used *p*-nitrosodimethylaniline (PDNA) as a reference system with the reference rate constant from Buxton.[3] However, almost all measured rates in the paper of Kwon[49] are slower than earlier data summarized in the review of Buxton[3] by approximately a factor of two. This might indicate a systematic problem in their approach. For the reaction of OH with benzoate, an average rate constant of $k = 5.9\times10^9$ M^{-1}s^{-1} is recommended as the average of the available rate constants with the exception of the Kwon[49] measurement, which is lower by about a factor of two as the only one of eight independent determinations.

As can be seen from Table 7, the situation for the reaction of OH with hydroxybenzoate is similar. Again the rate constants recently obtained by Kwon et al.[49] are much smaller than those found for 2-hydroxybenzoate by Amphlett et al.,[54] or those for 4-hydroxybenzoate found by Shetiya et al.[55] and Neta and Dorfmann.[56]

Monod et al.[28] stated in their paper that their rate constant for phenol is probably too low in comparison with the available literature values. Also other phenolic compounds react usually much faster with OH radicals. Therefore, it is recommended to use the older values reported in Table 7.

Inorganic compounds

Compared to the reaction of OH towards organic compound, only a few reactions with inorganic compound have been newly studied including rate constants for the OH reactions with chloride, bromide, iodide,[57] carbonate, bicarbonate, thiosulphate, sulfite, H_2O_2 and thiocyanate,[58] for all others Kwon et al.[49]

Kwon et al.[49] state that the rate constant of OH with chloride is 2.8×10^9 M^{-1}s^{-1} at pH 8.75. It has long been known that a direct oxidation of chloride by OH will only possible in acidic solution as this reaction is not a concerted one-step electron transfer, but a sequence of three coupled equilibria, one of which requires the reaction of a proton to lead to the release of a chlorine atom. This has been treated before in great detail, see Zellner and Herrmann[59] and references therein.

Finally, there are discrepancies for the reaction of OH with bromide (Table 8). Again, the recent determination by Kwon[49] is smaller than the classical determination by Zehavi and Rabani.[60] The reason for the discrepancy between both studies could be the pH dependency of the reaction rate constant as described in Matheson et al.[61]

Table 7. Summary of the available kinetic data measured for OH radical reactions with phenol, benzoate and hydroxybenzoates at $T = 298$ K in aqueous solution.

Technique	pH	k_{2nd} [M^{-1}s^{-1}]	Measuring technique	$k_{ref,298K}$ [M^{-1}s^{-1}]	Ref.
		Benzoate			
CFS/H_2O_2	8.7	$(2.5\pm1.6)\times10^9$	C.K./PNDA	1.25×10^{10}	[49]
PR	5–6	6.0×10^9	direct/PBK	–	[114]
PR	6	$(6.3\pm0.3)\times10^9$	C.K./ABTS	1.2×10^{10}	[115]
PR	7	5.7×10^9	direct/PBK	–	[116]
PR	6–9	6.1×10^9	C.K./$Fe(CN)_6^{4-}$	1.0×10^{10}	[117]
PR	7	5.7×10^9	direct/PBK	–	[117]
PR	6–9	6.0×10^9	direct/PBK	–	[56]
PR	6–7	5.5×10^9	direct/SCN^-	1.0×10^{10}	
		2-hydroxybenzoate			
CFS/H_2O_2	8.7	$(3.9\pm1.2)\times10^9$	C.K./PNDA	1.25×10^{10}	[49]
PR	7	1.2×10^{10}	direct/PBK	–	[54]
PR	7	2.0×10^{10}	direct/SCN^-	1.0×10^{10}	[54]
		4-hydroxybenzoate			
CFS/H_2O_2	8.7	$(2.3\pm0.4)\times10^9$	C.K./PNDA	1.25×10^{10}	[49]
PR	7	6.9×10^9	direct/PBK	–	[118]
GR	9	8.0×10^9	C.K./EtOH	1.9×10^9	[55]
PR	7	9.0×10^9	direct/PBK	–	[56]
		Phenol			
SPR/PhotoFenton	2	$(1.9\pm0.2)\times10^9$	C.K./2-PrOH	1.9×10^9	[28]
PR	7	6.6×10^9	direct/PBK	–	[119]
PR	7.6	1.4×10^{10}	direct/PBK	–	[120]
PR	6-7	1.8×10^{10}	direct/SCN^-	1.1×10^{10}	[73]

2.4. Review of the SCN^- Competition Kinetic Reference System

Usually, the preferred method to measure kinetic data is the direct measurement of concentration–time profiles of the reactants. However, due to the weak absorption of the OH radical in the UV range (see Section 2.2) and overlapping absorptions of the other reaction partners and/or reaction products it is not practicable to follow the OH radical decay directly. Another direct approach is the measurement of product build up kinetics. This method also requires a detailed understanding on possi-

Table 8. Summary of the available kinetic data measured for the reaction between OH and bromide at $T = 298$ K in aqueous solution.

Technique	pH	k_{2nd} [$M^{-1}s^{-1}$]	Measuring technique	$k_{ref,298K}$ [$M^{-1}s^{-1}$]	Ref.
CFS/H_2O_2	8.7	$(4.2\pm1.6)\times10^9$	C.K./PNDA	1.25×10^{10}	[49]
PR	1	1.1×10^{10}	C.K./EtOH	1.8×10^9	[60]

ble influences of co-absorbing species in the reaction solution as well as the further fate of the reaction product. Therefore, direct or at least semidirect measurements (with corrections for co-absorbing species) of OH radical rate constants in aqueous solution are restricted to a few studies only. Due to these difficulties in the direct measurements of OH radical reactions competition kinetic methods using different reference systems are widely applied. A good reference system should fulfill the following requirements: 1) a well-characterized OH radical rate constant of the reference reaction, 2) well-characterized follow-up chemistry of the reference system, 3) fast, easy and distinct measurement technique for the reference reaction kinetics, 4) no influences of the reference system on the rate of the investigated reaction. In the past decades several reference compounds such as propanol, methanol, nitrobenzene, *p*-nitrosodimethylaniline (PNDA) and 4-chloro-3,5-dinitrobenzoic acid (CDNBA) have been applied for competition kinetic measurements.[3,28,49,50] The most commonly used and best characterized reference system is the thiocyanate (SCN^-) system. However, the reference system itself is still under investigation and different reference rate constants have been applied by the different groups. Therefore, the applied reference rate constants should be always included in the discussion when results of different studies are compared. Looking at the reference rate constants applied in studies since 2003 (Table 9), differences in the obtained kinetic data of up to 50% can be explained only by the usage of different reference rate constants for the thiocyanate system. For this reason all the reference rate constants applied in the different studies are included in Table 9. A short review on the state of the art of the thiocyanate system is given in the following.

Kinetics

The chemistry following the reaction of SCN^- with OH radicals in neutral or acidic solution is shown in the following sequence (R2–R4)[68]. For kinetic measurements the formed $(SCN)_2^-$ concentration is detected in the reaction solution by absorption measurements. The absorption spectrum of the $(SCN)_2^-$ radical anion is shown and reviewed in the following section. It is assumed that each OH radical reacts with one SCN^- leading to the formation of one $(SCN)_2^-$ radical anion in absence of other potential reaction partners. Adding reactants to the measure-

Table 9. Summary of the available kinetic data describing the thiocyanate (SCN^-) reference system for competition kinetics.

	Technique	pH	k_{2nd}	K	A	E_A kJ mol^{-1}	Measuring technique	$k_{ref,298K}$ $M^{-1}s^{-1}$	Ref.
$OH + SCN^- \xrightarrow{k_2} SCNOH^-$									
k_2	PR		6.6×10^9 $M^{-1}s^{-1}$		–	–	PBK/$(SCN)_2^-$	–	[73]
k_2	PR		2.0×10^{10} $M^{-1}s^{-1}$		–	–	PBK/$(SCN)_2^-$	–	[65]
k_2	PR		2.8×10^{10} $M^{-1}s^{-1}$		–	–	PBK/$(SCN)_2^-$	–	[66]
k_2	PR		1.0×10^{10} $M^{-1}s^{-1}$		–	–	C.K./EtOH	1.9×10^9	[121]
k_2	PR		1.1×10^{10} $M^{-1}s^{-1}$		–	–	C.K./MeOH	9.7×10^8	[121]
k_2	PR		1.08×10^{10} $M^{-1}s^{-1}$		–	–	PBK/$(SCN)_2^-$	–	[67]
k_2	PR		1.0×10^{10} $M^{-1}s^{-1}$		–	–	PBK/$(SCN)_2^-$	–	[122]
k_2	PR		1.1×10^{10} $M^{-1}s^{-1}$		9.6×10^{11} $M^{-1}s^{-1}$	10.9	C.K./$HCOO^-$	4.1×10^9	[63]
k_2	PR		9.6×10^9 $M^{-1}s^{-1}$		1.8×10^{12} $M^{-1}s^{-1}$	12.6	C.K./*t*BuOH	7.3×10^8	[63]
k_2	FP		1.24×10^{10} $M^{-1}s^{-1}$		7.3×10^{12} $M^{-1}s^{-1}$	15.8	PBK/$(SCN)_2^-$	–	[62]
k_2	GR		1.2×10^{10} $M^{-1}s^{-1}$		–	–	C.K./$C_6H_5CO_2^-$	$5.9\cdot10^9$	[123]
k_2	FP		1.2×10^{10} $M^{-1}s^{-1}$		3.1×10^{12} $M^{-1}s^{-1}$	13.7	PBK/$(SCN)_2^-$	–	[124]
k_2			1.2×10^{10} $M^{-1}s^{-1}$		3.6×10^{12} $M^{-1}s^{-1}$	14.1	averaged from[63] and[62]	–	[31]
k_2	PR		1.4×10^{10} $M^{-1}s^{-1}$		–	–		–	[58]
k_2			1.1×10^{10} $M^{-1}s^{-1}$		–	–	selected value	–	[3]
k_2			1.13×10^{10} $M^{-1}s^{-1}$		–	–	average	–	this work
$SCNOH^- \underset{k_{-3}}{\overset{k_3}{\rightleftharpoons}} OH^- + SCN$									
				3.2×10^{-2} M					[68]
k_3		≤ 7	$k_3 \gg k_2[SCN^-]$						[68]
k_3		>7	$>5\times10^7$ s^{-1}						[68]
k_{-3}		>7	$>1.5\times10^9$ $M^{-1}s^{-1}$						[68]
$SCN + SCN^- \underset{k_{-4}}{\overset{k_4}{\rightleftharpoons}} (SCN)_2^-$									
				2.0×10^5 M^{-1}					[68]
				1.9×10^5 M^{-1}					[62]
				1.8×10^5 M^{-1}					[62]
									[125]
k_4	PR		6.6×10^9 $M^{-1}s^{-1}$		–	–	PBK/$(SCN)_2^-$	–	[64, 70]
k_4	PR		7.0×10^9 $M^{-1}s^{-1}$		–	–	PBK/$(SCN)_2^-$	–	[66]
k_4	PR		1.08×10^{10} $M^{-1}s^{-1}$		–	–	PBK/$(SCN)_2^-$	–	[67]
k_4	PR		6.9×10^9 $M^{-1}s^{-1}$		1.5×10^{10} $M^{-1}s^{-1}$	2.2	PBK/$(SCN)_2^-$	–	[62]

ment solution decreases the amount of $(SCN)_2^-$ formed in dependence of the reactant concentration and its reactivity towards OH (R5):

$$H_2O_2 + h\nu \rightarrow 2\,OH \quad (R1)$$

$$OH + SCN^- \rightleftharpoons SCNOH^- \quad (R2)$$

$$SCNOH^- \rightleftharpoons SCN + OH^- \quad (R3)$$

$$SCN + SCN^- \rightleftharpoons (SCN)_2^- \quad (R4)$$

$$OH + \text{reactant} \rightarrow \text{products} \quad (R5)$$

Therefore, measuring the $(SCN)_2^-$ absorptions ($A_{[(SCN)_2^-]}x$) in dependence of the added reactant concentration allows the calculation of k_5 by applying Equation (1):

$$\frac{A_{[(SCN)_2^-]_0}}{A_{[(SCN)_2^-]_x}} = \frac{k_5[\text{reactant}]}{k_2[SCN^-]} + 1 \quad (1)$$

The thiocyanate reference system is probably the best characterized reference system currently applied in the literature. However, there are still uncertainties in the measured rate constants of the single reactions in the reference system (R2–R4). Available rate constants concerning the SCN^- reference system are listed in the following Table 9.

As can be seen from the data of Table 9 different reference rate constants for reaction R2 are applied in the literature. This aspect needs to be considered when rate constants from different studies are compared. Therefore, a widely accepted rate constant for R2 that simplifies the comparison of kinetic data from different groups should be defined based on the existing studies. A first approach in this direction was done by Buxton in 1988[3] by selecting a value of $k_2 = 1.1\times10^{10}$ $M^{-1}s^{-1}$ for R2. However, since that time a number of additional studies were published in the literature reporting larger rate constants. Zhu et al.[31] averaged the temperature-dependent rate constants from two studies[62,63] and applied the mean values in their study (Figure 3). Both studies were weighted equally with the exception that the values at the highest temperatures (T = 352 K) from Elliot and Simsons[63] were not included. Since the temperature dependency of R2 was not further investigated in the last years the mean temperature dependency calculated by Zhu in 2003[31] is still valid. However, as can be seen in Figure 3, if one applies the temperature dependency from Zhu[31], from Chin and Wine[62] or from Elliot and Simsons,[63] it will not affect the results strongly.

Based on the data compilation in Table 9 an average rate constant for R2 at T = 298 K was calculated and included in Table 9. The averaged value includes almost all rate constants listed in Table 9 with the following exceptions. The selected value from Buxton[3] was not considered since it is an averaged and not an experimentally obtained value. Furthermore, the value from Adams[64] was not included since it was later shown by Baxendale[65] that the reported value from Adams refers to R4 rather than to R2. The reported rate constant for R2 from Baxendale 1967[65] and 1968[66] is significantly larger than all the other available rate constants for reaction R2. Therefore,

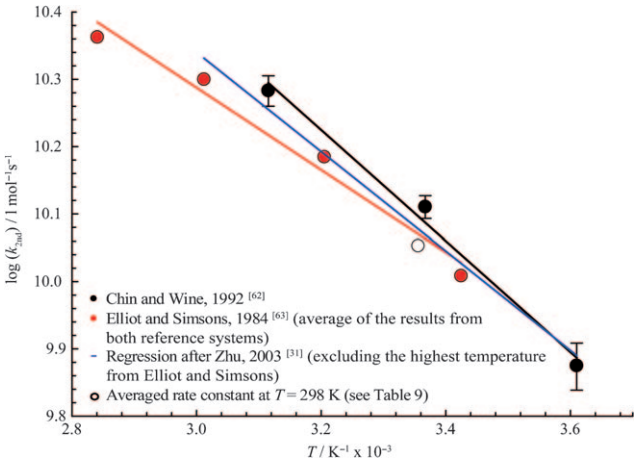

Figure 3. Measured and averaged temperature dependences for the reaction between OH and SCN^- reported in the literature.

these values were also excluded for the averaging. The averaged rate constant obtained of $k_{2,aver} = 1.13\times10^{10}$ $M^{-1}s^{-1}$ confirms the selected value from Buxton[3] and fits well into the averaged temperature dependency from Zhu et al.[31] (Figure 3).

The lifetime of the $SCNOH^-$ complex formed in R2 is extremely short (~5 ns) and exact rate constant measurements are sparse. It was assumed that the reverse reaction of R3 can be neglected in acidic solutions.[67,68] Only Behar and co-workers[68] report a lower limit for R3 of $k_3 > 5\times10^7$ s^{-1} and $k_{-3} > 1.5\times10^9$ $M^{-1}s^{-1}$ in alkaline solution.

The temperature-dependent measurement of k_4 by Chin and Wine [62] is the only one available in the literature. The measured rate constant at T = 297 K does agree quite well with the available literature values measured at the same temperature. However, the other measured rate constants k_4 at T = 277 K and T = 321 K does not give a good linear relationship according to the Arrhenius law. Therefore, the reported activation energy and pre-exponential factor in Table 9 contains large errors. For the kinetic investigations the peak absorbance (A_t) of $(SCN)_2^-$ at a certain wavelength is measured. Since the decay of $(SCN)_2^-$ is much slower than its formation, the measured peak absorbance A_t is almost equal to the maximal $(SCN)_2^-$ concentration in the reaction solution. The peak absorbance of $(SCN)_2^-$ is reached after approximately 5 μs according to the study of Milosavljevic and LaVerne.[58] Sink reactions for the $(SCN)_2^-$ radical anion in aqueous solution are recombination reactions or the reaction with the SCN radical (Table 10).[58,62,66,69]

An effect which could influence the measured peak absorbance of $(SCN)_2^-$ in laser photolysis experiments when H_2O_2 is applied as radical precursor are absorptions of the added reactants at the H_2O_2 photolysis wavelength. Co-absorbers could influence the amounts of formed OH radicals by R1. This can theoretically affect the concentrations of $(SCN)_2^-$ in parallel to reaction R5. However, only strong absorbing reactants could potentially influence the results of the kinetic measurements leading to an overestimation of the rate constants. In such

cases reactant concentrations should be minimized in order to keep this effect small.

Another aspect of the thiocyanate reference system which needs to be considered in some applications, is the formation of $(SCN)_2^-$ radicals from the laser photolysis of SCN^- itself. It is known that SCN^- photolysis can lead to the formation of SCN radicals which will further react to $(SCN)_2^-$ radicals (R4).[70,71] However, the measured quantum yield at $\lambda = 248$ nm for reaction R6 ($\Phi < 0.02$) is small.[70–72]

Table 10. Summary of kinetic data describing the self-reaction of $(SCN)_2^-$ radical anions in aqueous solution.

	Technique	k_{2nd}	Ref.
$2(SCN)_2^- \xrightarrow{k_6} (SCN)_2 + 2SCN^-$			
$2k_6$	PR	1.2×10^9 M^{-1}s^{-1}	[126]
$2k_6$	PR	2.6×10^9 M^{-1}s^{-1}	[76]
$2k_6$	PR	2.0×10^9 M^{-1}s^{-1}	[125]
$2k_6$	PR	1.2×10^9 M^{-1}s^{-1}	[58]

$$SCN^- + h\nu \rightarrow SCN + e^- \quad (R6)$$

$$SCN^- + h\nu \rightarrow CN^- + S \quad (R7)$$

Therefore, the amount of formed $(SCN)_2^-$ by this channel is usually low. An significant formation of $(SCN)_2^-$ from the SCN^- photolysis would increase the ratio $\left(A_{[(SCN)_2^-]_0} / A_{[(SCN)_2^-]_x}\right)$ in Equation (1) with increasing reactant concentration and subsequently overestimate the rate constant for R5. But, due to the small quantum yield of R6 at $\lambda = 248$ nm, this effect should be insignificant for the kinetic measurements using the laser photolysis technique. However, precise OH radical concentration measurements as needed for example for quantum yield calculations based on the SCN^- system should correct for this additional $(SCN)_2^-$ source. Available literature data on the $(SCN)_2^-$ absorption spectra are summarized and discussed in the following chapter.

Spectra

While the knowledge of the exact extinction coefficient of the $(SCN)_2^-$ radical anion for the competition kinetic studies are of minor importance, these data are needed when the SCN^- system is used to measure OH radical concentrations or as dosimeter for pulse radiolysis experiments. The available absorption spectra are summarised in Figure 4.

The absorption spectra of $(SCN)_2^-$ was measured by different groups over the last five decades. Starting with the studies from Adams and coworkers in 1965[64,73,74] the absorption spectra of $(SCN)_2^-$ and other transients in the SCN^- system have been measured until today in order to characterize this important and widely used reference system. In order to calculate extinction coefficients of $(SCN)_2^-$ both the chemistry going on after the reaction of SCN^- with OH as well as the further reactions of $(SCN)_2^-$ needs to be known. Most of the studies included in Figure 4 measured only the absorption spectra of $(SCN)_2^-$ and did not calculate the corresponding extinction coefficients. They used usually known extinction coefficients of former studies in order to get this data.

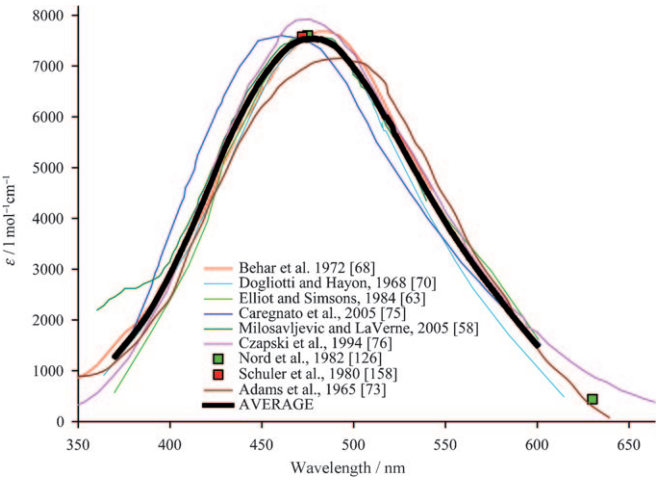

Figure 4. Compilation of digitized $(SCN)_2^-$ radical anion absorption spectra in aqueous solution. The data table of the averaged $(SCN)_2^-$ spectra is given in the Supporting Information (Table S2).

Even if the spectra agree in general well, slight differences can be seen which could be of importance for spectroscopic studies. With the exception of Adams et al.[74] and Caregnato et al.[75] the maximum absorption is found around $\lambda \approx 478$ nm. In the study of Caregnato and coworkers[75] the whole absorption band is blue-shifted by approximately 15 nm. The spectra published by Czapski et al.[76] shows a higher absorption at the peak absorbance. They calculated the extinction coefficient and reported an extinction coefficient in the maximum of $\varepsilon_{472nm} = 7950$ M^{-1}cm^{-1}. This value is about 5% higher than the averaged extinction coefficient of all spectra in Figure 4 at the same wavelength.

All spectra published in the literature we digitized using the Engauge Digitizer (Version 4.1) program. If no extinction coefficients (ε) are plotted in the papers, ε was calculated using the reported extinction coefficients for a certain wavelength (normally the absorption maximum) published herein. Subsequently all scanned data were plotted and smoothed with SigmaPlot 10 software. The smoothed data pairs of all digitized spectra were averaged. The calculated data points including standard deviations are given in Table S2 in the Supporting Information. Digitized spectra including the average spectrum are shown in Figure 4.

3. The Nitrate (NO_3) Radical

3.1. Overview

The nitrate radical is an important night-time oxidant in all tropospheric compartments. It is mainly formed from the gas-phase reaction between NO_2 and ozone.[77] In contrast to the OH radical there are almost no atmospherically relevant direct

sources for NO_3 in aqueous solution. Only electron transfer reactions between nitrate anions and radicals such as SO_x^- can contribute to the NO_3 radical budget in clouds and deliquescent particles. Therefore, transfer from the gas phase is considered as the most important source for NO_3 becoming active in aqueous solution reactions in the troposphere. The phase transfer of NO_3 has been described by a number of authors, with the latest studies by Rudich et al.[78] and Schütze and Herrmann.[79]

Applying the CAPRAM mechanism in its current version gives the following NO_3 concentrations in warm clouds and deliquescent particles. NO_3 concentrations in Table 11 have been calculated for three different cases (urban, remote and maritime). The calculated NO_3 radical concentrations vary strongly between the six different cases as it has been observed for OH before. A comparison with OH reveals much higher NO_3 cloud water concentrations in the urban scenario. These results indicate the importance of NO_3 oxidation reactions for the atmospheric chemistry at night. In the other considered scenarios the calculated NO_3 concentrations are usually lower than the calculated OH values. Furthermore, in contrast to OH and SO_4^-, NO_3 radicals show the highest concentrations in the urban scenario because of the enhanced precursor concentrations in this scenario. As can be seen in Figure S1 in the Supporting Information, the NO_3 diurnal cycles are complementary to those of OH and NO_3 peak concentrations are reached during nighttime (Figure S1).

On the experimental side, it is much easier to measure NO_3 radical concentrations directly due to the typical absorptions of the nitrate radical above 600 nm, which do not change much when the gas phase and the aqueous solution spectra are compared. Typically, NO_3 radical concentration changes are followed at 635 nm using cw diode lasers or helium-neon lasers. The earlier techniques of NO_3 generation in aqueous solution have been discussed by Herrmann and Zellner, 1998[5] and there is a single development in the generation of NO_3 which applies the conversion of OH:

$$NO_3^- + H^+ + h\nu \rightarrow NO_2 + OH \quad (R8)$$

$$OH + HNO_3 \rightarrow NO_3 + H_2O \quad (R9)$$

This method uses the reaction of OH with HNO_3 which is well-known from gas phase chemistry but occurs in the same manner in aqueous solution provided the solution is acidic enough to contain considerable amount of undissociated nitric acid, so that the application is restricted to pH values below pH 1. The method has been introduced as the existing other methods to generate NO_3 in aqueous solution do all make use of highly oxidizing precursors, that is, either peroxodisulphate or cerium(IV) nitrate which are both well-known oxidizers in the chemical laboratory, preventing kinetic studies of the reactions of NO_3 with reactants which could be oxidized, such as phenols. The method has been introduced in the study by Umschlag et al.[80] and has been further used to study phenolic compounds since then.[81–83] The absorption spectrum of NO_3 has also been discussed in Herrmann and Zellner[5] and there are no more recent measurements since that discussion.

Reaction mechanisms of NO_3 radical reactions includes H-abstraction reactions and addition reactions to C=C double bonds where the reaction follow a similar mechanism as their OH equivalents and as known from the gas phase. A recent reactivity comparison can be found in Hoffmann et al.[24]

NO_3 can undergo direct electron transfer reactions with inorganic anions, carboxylate anions, and electron rich aromatic compounds where it is much more reactive than OH as indicated by its much higher one electron reduction potential of 2.41 V against 1.90 V for OH.[84]

3.2. NO_3 Kinetics

The existing kinetic dataset for aqueous NO_3 reactions is much smaller compared to the large compilation for OH radical reactions, which may be due to the lower reactivity of NO_3. Therefore, numerous rate constants even for smaller organic reactants are currently missing in the literature. Data compilations of NO_3 radical reactions can be found in Neta et al.,[4] Herrmann and Zellner,[5] the NIST Solution Kinetics Database 3.0[6] and Herrmann.[7] It appears that since the last review, only three different laboratories published new atmospherically relevant NO_3 kinetic data in aqueous solution. These data are mainly for reactions with carboxylic acids, polyfunctional alcohols as well as substituted phenolic compounds. Structure–activity relationships and computerized pathway elucidation modules as established for OH radical reactions are not reported for NO_3 aqueous phase reactions so far. However, for the prediction of kinetic data Evans–Polanyi-type reactivity correlations can be used for reactions following an H-abstraction mechanism. The latest version of this reactivity correlation is reported in Hoffmann et al.[24] and is discussed in a later section. The same indexing is applied for the NO_3 kinetic data (Table 12) as for the OH reactions in Table 2.

Table 11. Calculated NO_3 radical concentrations in clouds and deliquescent particles using the CAPRAM 3.0i multiphase mechanism. Mean concentrations are averaged values over three simulation days.

	Urban case: $[NO_3]$ in mol L^{-1}			Remote case: $[NO_3]$ in mol L^{-1}			Maritime case: $[NO_3]$ in mol L^{-1}		
	mean	max	min	mean	max	min	mean	max	min
Cloud droplets	1.4×10^{-13}	2.7×10^{-13}	4.7×10^{-14}	5.1×10^{-15}	1.7×10^{-14}	1.1×10^{-15}	6.9×10^{-15}	2.0×10^{-14}	1.9×10^{-15}
Deliquescent particles	8.6×10^{-14}	2.1×10^{-13}	2.4×10^{-14}	3.5×10^{-13}	1.0×10^{-12}	8.0×10^{-16}	1.9×10^{-15}	6.7×10^{-15}	1.6×10^{-16}

Table 12. Compilation of newly measured aqueous phase NO_3 radical kinetic data relevant for atmospheric chemistry. Coding and abbreviations are explained in the text or below the Table.

Reactant	Technique	pH	k_{2nd} [$M^{-1}s^{-1}$]	Comments	A [$M^{-1}s^{-1}$]	E_A [$kJ\,mol^{-1}$]	Measuring technique	Ref.
Aliphatic alcohols								
1,2-ethanediol	LFP/$S_2O_8^{2-}$	~6	$(6.6\pm2.8)\times10^6$	2, B*, □,○,■	$(7.1\pm1.1)\times10^9$	17.6 ± 8.3	direct/NO_3/635 nm	[24]
1,2-propanediol	LFP/$S_2O_8^{2-}$	~6	$(9.9\pm0.8)\times10^6$	1	$(6.8\pm0.2)\times10^{10}$	21.8 ± 2.3	direct/NO_3/635 nm	[24]
1,2,3-propanetriol	LFP/$S_2O_8^{2-}$	~6	$(1.3\pm0.2)\times10^7$	2, B, □,○	$(1.4\pm0.05)\times10^{12}$	28.7 ± 2.4	direct/NO_3/635 nm	[24]
erythritol	LFP/$S_2O_8^{2-}$	~6	$(1.4\pm0.2)\times10^7$	1	$(3.4\pm0.2)\times10^{10}$	19.3 ± 3.4	direct/NO_3/635 nm	[24]
arabitol	LFP/$S_2O_8^{2-}$	~6	$(1.5\pm0.3)\times10^7$	1	$(1.1\pm0.1)\times10^{10}$	16.6 ± 3.6	direct/NO_3/635 nm	[24]
mannitol	LFP/$S_2O_8^{2-}$	~6	$(1.4\pm0.2)\times10^7$	1	$(5.1\pm0.6)\times10^{10}$	20.5 ± 6.6	direct/NO_3/635 nm	[24]
levoglucosan	LFP/$S_2O_8^{2-}$	~6	$(1.6\pm0.2)\times10^7$	1	$(2.3\pm0.1)\times10^{10}$	17.8 ± 2.6	direct/NO_3/635 nm	[110]
Carboxylic acids								
propionic acid	TWG/$S_2O_8^{2-}$	1	$(7.7\pm0.2)\times10^4$	1	–	–	direct/NO_3/635 nm	[127]
pyruvic acid	LFP/$S_2O_8^{2-}$	6	$(2.4\pm0.3)\times10^6$	1	$(8.8\pm0.6)\times10^8$	15 ± 4	direct/NO_3/635 nm	[82]
pyruvate	LFP/$S_2O_8^{2-}$	0.5	$(1.9\pm0.5)\times10^7$	1	$(3.7\pm0.3)\times10^{11}$	24 ± 5	direct/NO_3/635 nm	[82]
lactic acid	LFP/$S_2O_8^{2-}$	6	$(2.1\pm0.9)\times10^6$	1	$(1.0\pm0.3)\times10^{11}$	27 ± 20	direct/NO_3/635 nm	[82]
lactate	LFP/$S_2O_8^{2-}$	0.5	$(1.0\pm0.2)\times10^7$	1	$(8.3\pm0.4)\times10^{10}$	22 ± 3	direct/NO_3/635 nm	[82]
glycolic acid	LFP/$S_2O_8^{2-}$	6	$(9.1\pm2.3)\times10^5$	1	$(4.5\pm1.0)\times10^{11}$	33 ± 14	direct/NO_3/635 nm	[82]
glycolate	LFP/$S_2O_8^{2-}$	0.5	$(1.0\pm0.2)\times10^7$	1	$(1.8\pm0.3)\times10^{11}$	25 ± 9	direct/NO_3/635 nm	[82]
malonic acid	TWG/$S_2O_8^{2-}$	0.3	$(5.1\pm0.1)\times10^4$	1	–	–	direct/NO_3/633 nm	[128]
malonate (mono-anion)	TWG/$S_2O_8^{2-}$	4.26	$(5.6\pm2.1)\times10^6$	1	$(5.0\pm0.6)\times10^{11}$	28 ± 7	direct/NO_3/633 nm	[128]
malonate (di-anion)	TWG/$S_2O_8^{2-}$	8	$(2.3\pm0.5)\times10^7$	1	$(6.3\pm0.8)\times10^{11}$	25 ± 8	direct/NO_3/633 nm	[128]
mesoxalic acid	TWG/NO_3^-	0	$(1.7\pm0.5)\times10^6$	1	$(5.1\pm0.4)\times10^8$	13 ± 4	direct/NO_3/633 nm	[128]
mesoxalate (mono-anion)	TWG/$S_2O_8^{2-}$	2.7	$(2.3\pm0.4)\times10^7$	1	–	–	direct/NO_3/633 nm	[128]
mesoxalate (di-anion)	TWG/$S_2O_8^{2-}$	8	$(4.9\pm1.5)\times10^7$	1	$(1.4\pm0.1)\times10^{12}$	26 ± 4	direct/NO_3/633 nm	[128]
oxalic acid	PR	<0	$(2.4\pm0.2)\times10^4$	1	–	–	direct/NO_3/630 nm	[129]
oxalate (mono-anion)	TWG/$S_2O_8^{2-}$	2.7	$(4.4\pm0.2)\times10^7$	1	–	–	direct/NO_3/633 nm	[128]
	PR	3	$(7.8\pm0.7)\times10^7$	1	–	–	direct/NO_3/630 nm	[129]
oxalate (di-anion)			$(2.2\pm0.8)\times10^8$	1	$(2.2\pm0.2)\times10^{12}$	23 ± 6	direct/NO_3/633 nm	[128]
	PR	7	$(2.2\pm0.1)\times10^8$	1	–	–	direct/NO_3/630 nm	[129]
succinic acid	TWG/$S_2O_8^{2-}$	0.3	$(5.0\pm5.0)\times10^3$	1	–	–	direct/NO_3/633 nm	[128]
succinate (mono-anion)	TWG/$S_2O_8^{2-}$	4.2	$(1.1\pm0.2)\times10^7$	1	–	–	direct/NO_3/633 nm	[128]
succinate (di-anion)	TWG/$S_2O_8^{2-}$	8	$(1.8\pm0.2)\times10^7$	1	$(6.2\pm0.6)\times10^{11}$	26 ± 3	direct/NO_3/633 nm	[128]
Oxygenated compounds								
2-butanone	LFP/NO_3^-	0.5	$(2.2\pm0.4)\times10^7$	1	$(3.9\pm0.9)\times10^{11}$	24 ± 15	direct/NO_3/635 nm	[82]
hydroxyacetone	LFP/NO_3^-	0.5	$(1.8\pm0.3)\times10^7$	1	$(4.0\pm0.8)\times10^9$	13 ± 11	direct/NO_3/635 nm	[82]
propionaldehyde	LFP/NO_3^-	0.5	$(5.8\pm1.6)\times10^7$	1	$(3.2\pm0.5)\times10^{11}$	22 ± 11	direct/NO_3/635 nm	[82]
butyraldehyde	LFP/NO_3^-	0.5	$(5.6\pm2.3)\times10^7$	1	$(4.9\pm0.4)\times10^{10}$	17 ± 4	direct/NO_3/635 nm	[82]
t-butylmethylether	TWG/$S_2O_8^{2-}$	1	$(3.9\pm1.3)\times10^5$	1	–	–	direct/NO_3/635 nm	[127]
dimethylsuccinate	TWG/$S_2O_8^{2-}$	1	$(3.4\pm0.2)\times10^4$	1	–	–	direct/NO_3/635 nm	[127]
diethylcarbonate	TWG/$S_2O_8^{2-}$	1	$(8.4\pm1.3)\times10^4$	1	–	–	direct/NO_3/635 nm	[127]
dimethylcarbonate	TWG/$S_2O_8^{2-}$	1	$(1.5\pm0.4)\times10^4$	1	–	–	direct/NO_3/635 nm	[127]
dimethylmalonate	TWG/$S_2O_8^{2-}$	1	$(2.6\pm0.7)\times10^4$	1	–	–	direct/NO_3/635 nm	[127]
Aromatic compounds								
2,6-dichlorophenol	LFP/NO_3^-	0.5	$(1.3\pm0.2)\times10^9$	1	$(3.9\pm0.3)\times10^{11}$	21 ± 9	direct/NO_3/635 nm	[83]
2,6-dihydroxyphenol	LFP/NO_3^-	0.5	$(1.7\pm0.2)\times10^9$	1	$(6.9\pm0.6)\times10^{10}$	9 ± 5	direct/NO_3/635 nm	[83]
2,6-dimethylphenol	LFP/NO_3^-	0.5	$(1.8\pm0.3)\times10^9$	1	$(1.5\pm0.1)\times10^{12}$	17 ± 6	direct/NO_3/635 nm	[83]
2,6-dimethoxyphenol	LFP/NO_3^-	0.5	$(1.6\pm0.4)\times10^9$	1	$(1.0\pm0.1)\times10^{12}$	16 ± 7	direct/NO_3/635 nm	[83]
2,6-dinitrophenol	LFP/NO_3^-	0.5	$(2.8\pm0.9)\times10^8$	1	$(3.2\pm0.4)\times10^{11}$	18 ± 9	direct/NO_3/635 nm	[83]
4-hydroxy-3,5-dimethoxybenzaldehyde	LFP/NO_3^-	0.5	$(1.7\pm0.3)\times10^9$	1	$(2.8\pm0.2)\times10^{12}$	18 ± 4	direct/NO_3/635 nm	[83]
4-hydroxy-3,5-dimethoxybenzoic acid	LFP/NO_3^-	0.5	$(1.4\pm0.6)\times10^9$	1	$(2.8\pm0.4)\times10^{12}$	19 ± 10	direct/NO_3/635 nm	[83]
4-hydroxy-3-methoxybenzaldehyde	LFP/NO_3^-	0.5	$(1.1\pm0.2)\times10^9$	1	$(7.8\pm0.4)\times10^{11}$	16 ± 4	direct/NO_3/635 nm	[83]
4-hydroxy-3-methoxybenzoic acid	LFP/NO_3^-	0.5	$(1.0\pm0.3)\times10^9$	1	$(3.8\pm0.3)\times10^{11}$	15 ± 4	direct/NO_3/635 nm	[83]
3-hydroxy-4-methoxybenzoic acid	LFP/NO_3^-	0.5	$(1.3\pm0.4)\times10^9$	1	$(9.0\pm0.6)\times10^{10}$	11 ± 4	direct/NO_3/635 nm	[83]
4-methylphenol	LFP/NO_3^-	0.5	$(1.7\pm0.3)\times10^9$	2, B, ●	$(1.8\pm0.06)\times10^{10}$	6 ± 2	direct/NO_3/635 nm	[83]
4-methoxyphenol	LFP/NO_3^-	0.5	$(2.5\pm0.4)\times10^9$	2, B, ●	$(8.6\pm4.1)\times10^{11}$	15 ± 3	direct/NO_3/635 nm	[83]
4-hydroxybenzoic acid	LFP/NO_3^-	0.5	$(1.5\pm0.4)\times10^9$	2, B, ●	$(3.1\pm0.2)\times10^{11}$	13 ± 4	direct/NO_3/635 nm	[83]
4-nitrophenol	LFP/NO_3^-	0.5	$(8.8\pm4.6)\times10^8$	2, A, ●	-	-	direct/NO_3/635 nm	[83]
2-nitrophenol	LFP/NO_3^-	0.5	$(8.3\pm1.4)\times10^8$	2, B, ●	-	-	direct/NO_3/635 nm	[83]
4-aminophenol	LFP/NO_3^-	0.5	$(2.0\pm0.3)\times10^9$	2, B, ●	$(10.6\pm0.5)\times10^{10}$	10 ± 3	direct/NO_3/635 nm	[83]

PR = Pulse radiolysis; LFP = Laser flash photolysis; TWG = Teflon waveguide; □ Neta et al., 1988[4]; ○ NIST[6]; ■ Herrmann and Zellner, 1998[5]; ● Herrmann, 2003[7]

Aliphatic alcohols

Similar as for OH, there are new data on some polyalcohols and sugars, most of which are new temperature-dependent measurements. There are differences in the available data for the reactions of NO_3 with 1,2-ethanediol and 1,2,3-propanetriol, which are discussed in the following (Table 13).

Table 13. Summary of the available kinetic data measured for NO_3 radical reactions with 1,2-ethanediol and 1,2,3-propanetriol at $T = 298$ K in aqueous solution.

Technique	pH	k_{2nd} [$M^{-1} s^{-1}$]	Measuring technique	Ref.
		1,2-ethanediol		
LFP/$S_2O_8^{2-}$	~6	$(6.6\pm2.8)\times10^6$	direct/NO_3/635 nm	[24]
LFP/$K_2[Ce(NO_3)_6]$	<0	7.6×10^5	direct/NO_3/635 nm	[85]
PR	<0	1.6×10^6	direct/NO_3/600 nm	[86]
		1,2,3-propanetriol		
LFP/$S_2O_8^{2-}$	~6	$(1.3\pm0.2)\times10^7$	direct/NO_3/635 nm	[24]
PR	<0	1.8×10^6	direct/NO_3/600 nm	[86]
Averaged value		7.4×10^6		

The available rate constants on this reaction are all scattered. The greatest difference in these three studies is the pH of the measurement solution. Ito et al.[85] as well as Pikaev et al.[86] did apply extremely acidic solutions. It is not clear if the rate constants of this particular reaction can be affected by such drastic measurement conditions. However, the value from Hoffmann et al.[24] perfectly fits in an existing correlation between the bond strength of the weakest H-bond in the molecules and the logarithmic rate constants per abstractable H-atom for NO_3 radical reactions.[24] This could indicate that the reaction is faster than measured by Ito et al.[85] and Pikaev et al.[86]

The different reaction conditions discussed before could also be the reason for the differences observed for the reaction of 1,2,3-propanetriol with NO_3 in aqueous solution. However, the larger rate constant from Hoffmann[24] is faster than expected from the above mentioned correlation presented in Hoffmann et al.[24] and the value from Pikeav et al.[86] is much slower than expected from this correlation. Therefore, it is suggested to apply a mean value of the data of Table 13 for this reaction.

Oxygenated Compounds

In this substance group there are a total of nine new measurements (see Table 12) of some simple organics including four temperature dependences and four esters.

Carboxylic and Dicarboxylic Acids

There is a kinetic dataset obtained since 2004 by two laboratories,[82,127–129] covering a total of 21 reactions including 12 temperature dependences covering the mono-acids propionic, glycolic, lactic, pyruvic, and mesoxalic acid and the C2–C4 dicarboxylic acids and the respective mono- and dianions where applicable.

Aromatic Compounds

The newly measured reactions between the NO_3 radical and different *para*-substituted phenols in Weller et al.[83] show some differences to the earlier published data in Umschlag et al.[80] and Barzaghi and Herrmann.[81] As very recently discussed by Weller and co-authors[83] the rate constants of reactions between the NO_3 radical and phenolic reactants are found to strongly depend on experimental conditions such as pH and ionic strength. Therefore, direct comparisons between data from different studies should be undertaken with great care if differing experimental conditions are applied. This is the case for the reactions in the following Table 14 were either the pH, the radical source or the ionic strength is different in all three cited studies. Due to the dependency of the results on the experimental conditions applied it is not recommended by the authors to simply average the available data. Users should rather check the experimental conditions applied in these studies and choose the data which was measured under the most relevant conditions for their applications.

Table 14. Summary of the available kinetic data measured for NO_3 radical reactions with substituted phenols at $T = 298$ K in aqueous solution.

Technique	pH	k_{2nd} [$M^{-1} s^{-1}$]	Measuring technique	Ref.
		4-methylphenol		
LFP/NO_3^-	0.5	$(1.7\pm0.3)\times10^9$	direct/NO_3/632.8 nm	[83]
LFP/NO_3^-	0.0	$(8.2\pm0.3)\times10^8$	direct/NO_3/632.8 nm	[80]
		4-methoxyphenol		
LFP/NO_3^-	0.5	$(2.5\pm0.4)\times10^9$	direct/NO_3/632.8 nm	[83]
LFP/$S_2O_8^{2-}$	4.0	$(8.2\pm0.3)\times10^8$	direct/NO_3/632.8 nm	[80]
		4-hydroxybenzoic acid		
LFP/NO_3^-	0.5	$(1.5\pm0.4)\times10^9$	direct/NO_3/632.8 nm	[83]
LFP/NO_3^-	0.0	$(5.0\pm1.3)\times10^8$	direct/NO_3/632.8 nm	[80]
		2-nitrophenol		
LFP/NO_3^-	0.5	$(8.3\pm1.4)\times10^8$	direct/NO_3/632.8 nm	[83]
LFP/NO_3^-	0.5	$(2.3\pm0.4)\times10^7$	direct/NO_3/632.8 nm	[81]
		4-aminophenol		
LFP/NO_3^-	0.5	$(2.0\pm0.3)\times10^9$	direct/NO_3/632.8 nm	[83]
LFP/NO_3^-	0.0	$(8.1\pm0.3)\times10^8$	direct/NO_3/632.8 nm	[80]

4. The sulphate SO_4^- Radical Anion

4.1. Overview

Sulphur-oxy radicals such as SO_4^- are formed through the oxidation chain of S(IV) in the atmospheric aqueous phase.[87,88] Reactions of SO_4^- with other atmospheric reactants could therefore interfere the S(IV) oxidation chain. Therefore, it is necessary to investigate and characterize the reactivity of this atmospheric oxidant in aqueous solution. The reactivity of SO_4^- radical anions in aqueous solution was topic of several studies over the last decades. However, the currently available kinetic data set on atmospheric relevant SO_4^- reactions is still

rather small in comparison to OH and many important atmospheric reactions are not characterized.

So far no direct measurements of atmospheric aqueous phase SO_4^- concentrations have been reported. The values presented in the following are assessed from a model study applying the multiphase mechanism CAPRAM in its latest version[1] (Table 15). The calculated SO_4^- concentrations in Table 15 are comparable to the calculated NO_3 values. Highest SO_4^- concentrations are calculated for the remote case.

SO_4^- radical anions are usually generated from peroxodisulphate anions ($S_2O_8^{2-}$). There are several techniques available to produce SO_4^- radicals out of aqueous peroxodisulphate solutions. Usually, laser flash photolysis of peroxodisulphate or the pulse radiolysis technique is applied. Also the thermal decomposition of $S_2O_8^{2-}$ is known as a source for SO_4^- radical anions which can be applied in batch reactor studies on longer timescales (Figure 5). SO_4^- has an absorption maximum between 440 nm and 450 nm, which often allows a direct measurement of the radical concentration decay for the kinetic evaluation.

The absorption spectrum of the sulphate radical anion has been discussed before,[89,90] which is also true for the effective quantum yields ($\Phi_{SO_4^-}$) of the photolytic generation of SO_4^- from peroxodisulphate photolysis.[12] There are two recent quantum yield determinations to be discussed which are not included in ref. [12]. Yu and Barker published in 2004[90] a value of $\Phi_{SO_4^-} = 2$ at a photolysis wavelength of $\lambda = 248$ nm in aqueous solution. This quantum yield is significantly higher than the latest reported value in Herrmann.[12] Furthermore, a value of $\Phi_{SO_4^-} = 0.52$ was published by Criquet and Vel Leitner in 2009.[91] Their value appears too low in this wavelength range in comparison to the other available data. However, all available quantum yields of the photolytic generation of SO_4^- are very scattered and the precision of the values depends both on the accuracy of the energy measurement system and exact concentration measurements. Therefore, further measurements or theoretical calculations are needed in order to describe this important radical formation process more precisely.

A compilation of available SO_4^- absorption spectra in aqueous solution is shown in Figure 5. All spectra show the peak absorbance of SO_4^- radicals around $\lambda = 450$ nm. However, calculated extinction coefficients in earlier studies of Dogliotti et al.[92] Hayon et al.[87] Heckel et al.[93] Lesigne et al.[94] and Roebke et al.[95] are much lower compared to the more recent values in Figure 5. The first ones who report a higher extinction coefficient at $\lambda = 450$ nm ($\varepsilon = 1600\ M^{-1}cm^{-1}$) were Chawla and Fessenden in 1975.[96] Their value was later confirmed by several studies in the last two decades. As also done for OH and $(SCN)_2^-$ an averaged SO_4^- spectra was calculated and included in Figure 5. For the calculation of this spectrum only the newer values have been considered. The averaged spectrum is shown in between 350 nm and 600 nm, due to the large discrepancies in the absorption measurements below 350 nm. Below 350 nm the absorption spectrum of SO_4^- radical shows a second shoulder. However, the shape of this shoulder is quite different in most of the studies included in Figure 5. The calculated data points of the averaged spectrum are given in the Supporting Information (Table S3). The peak absorbance of the averaged spectrum is at $\lambda = 445$ nm ($\varepsilon_{SO_4^-,445nm} = 1544\ M^{-1}cm^{-1}$).

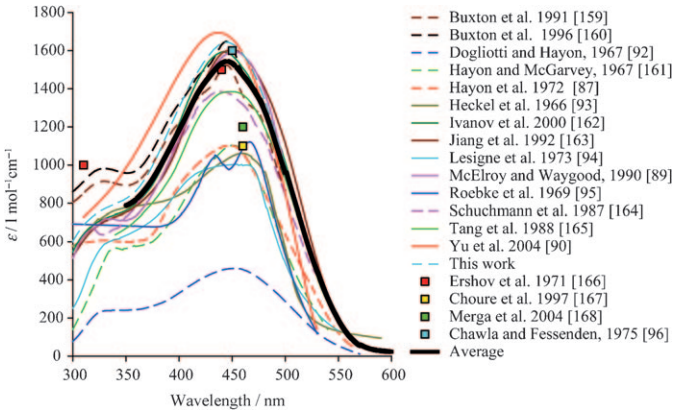

Figure 5. Compilation of digitized SO_4^- radical anion absorption spectra in aqueous solution. The data table of the averaged SO_4^- spectra is given in the Supporting Information (Table S3).

In many studies White cell optics in combination with an analytical cw laser or a lamp are applied for the measurement of the concentration-time profiles. The reactivity of SO_4^-, which is a strong one-electron oxidant, with organic reactants is usually considerably lower than OH, but on average higher than NO_3. However, the size of these reactivity differences strongly depends on the type of the organic reactant and the underlying reaction mechanism. The possible reaction mechanisms of SO_4^- are similar to the NO_3 radical and include the H-abstraction reactions, addition reactions, and the direct electron transfer reaction where the sulphate radical anion can be very effective with its reported one-electron reduction potential of $E^\circ = 2.44$ V.[84]

4.2. SO_4^- Kinetics

An overview over the existing kinetic data of SO_4^- reactions in aqueous solution is given in Neta et al.,[4] the NIST Solution Kinetics Database 3.0[6] and Herrmann.[7] Since this last review in

Table 15. Calculated SO_4^- radical concentrations in clouds and deliquescent particles using the CAPRAM 3.0i multiphase mechanism. Mean concentrations are averaged values over three simulation days.

	Urban case: $[SO_4^-]$ in mol L^{-1}			Remote case: $[SO_4^-]$ in mol L^{-1}			Maritime case: $[SO_4^-]$ in mol L^{-1}		
	mean	max	min	mean	max	min	mean	max	min
Cloud droplets	1.1×10^{-14}	2.8×10^{-14}	6.5×10^{-15}	2.4×10^{-14}	1.8×10^{-13}	4.0×10^{-15}	2.3×10^{-15}	5.7×10^{-14}	5.5×10^{-17}
Deliquescent particles	9.3×10^{-15}	4.8×10^{-14}	4.5×10^{-16}	3.6×10^{-13}	9.1×10^{-13}	1.6×10^{-15}	1.2×10^{-14}	1.2×10^{-13}	7.4×10^{-17}

2003, the reactivity of some new water-soluble organic reactants such as terpenes, alcohols, carboxylic acids and aromatic compounds was measured. These new kinetic data are summarized in Table 16. The data of Table 16 consist of measurements of aliphatic polyalcohols (3: diols and 4: sugars), carboxylic and dicarboxylic acids, their anions, mono-, and dianions as applicable with a total of thirteen species investigated. For the alcohols there are no literature data for comparison (category 1) and in the group of acid reactions there is one single former determination of group 2A for the malonate dianion. Temperature dependences have only been obtained for the alcohols.

Furthermore, new measurements are available for fifteen aromatic compounds with no temperature-dependent measurements, all of which fall into category 1 except for the reaction of the sulphate radical anion with benzene (see Table 17).

There are a total of five determinations for the rate constant of SO_4^- with benzene at room temperature, including three direct measurements utilising either pulse radiolysis [95,97] or laser photolysis.[98] The laser photolysis study resulted in a smaller rate constant than the former pulse radiolysis studies. Two further indirect studies appear to confirm a larger value of the rate constant.

There have been recent measurement of rate constants for the reactions of three sulphur-containing organics DMSO (indexed as 2A), $DMSO_2$ (index 1), MSA (1) the terpene and terpene-derivatives α-pinene (2B), myrtenal (2A), cis-pinonic acid (1) and isoprene (1). No temperature dependence is available. Deviations between available measurements do only exist for the reaction with α-pinene (Table 18). It may be speculated that a loss of the volatile α-pinene from the reactor in the determination of Zjajka and Pasiuk-Bronikowska[99] occurred. Possible error sources have been discussed by these authors.

Finally, a number of reactions of the sulphate radical anion with inorganic reaction partners have been studied consisting of the reaction with chloride, the self-reaction, the reaction with peroxodisulphate anions and the reaction with water. For all of these reactions former determinations exist and no drastic deviations against the former measurements are noted (index 2 A). Again, no temperature-dependent measurements are available.

5. Estimation Methods for Aqueous-Phase Kinetic Data

As stated in the introduction, a large number of experiments have been performed in order to determine the reaction kinetics of free radical reactions with organic and inorganic compounds relevant for the tropospheric multiphase chemistry. However, due to the innumerable quantity of organic compounds in troposphere it is impossible to experimentally determine all data needed to fully understand and implement the degradation mechanisms in explicit model applications. Therefore, several estimation methods such as structure–activity relationships (SARs) and empirical correlations have been developed and a few different approaches recently became available to predict missing kinetic data in aqueous solutions. The following chapter will outline the currently available estimation methods.

5.1. OH Radical

Due to the importance of the hydroxyl radical chemistry in the troposphere and in other fields of chemistry most of the estimation methods available now aim on the prediction of OH rate constants. While structure–activity relationships for the estimation of gas-phase kinetic data have already been established several years ago, corresponding aqueous-phase methods are still sparse. However, first approaches describing the reactivity of different compound classes have been published in the last years. These methods are presented in the following. Furthermore, the robustness of the three most easily applicable methods is compared and discussed.

In 2005 Monod et al.[28] presented a structure–activity relationship valid for H-abstraction reactions of alkanes, alcohols, aldehydes, ketones, acids, and ethers by OH radicals. In this method the molecule is split in increments based on the gas-phase approach of Atkinson[100] and its update by Kwok and Atkinson.[101] The method used as descriptors the group rate constants of the CH_X or hydroxyl groups k_{prim}, k_{sec}, k_{tert} and $k_{abst}(OH)$ to account for H-abstraction by OH radicals, which were modulated by a factor F accounting for the neighbouring effects of CH_x ($x=0$–3), alcohol, carbonyl, acid, or ether groups in α-position. The method could predict the reactivity of 84% of the tested compounds within a factor of 5.

Later, Monod and Doussin (2008)[102] refined the method for alkanes, alcohols, and carboxylic acids introducing new descriptors accounting for the neighbouring effects of functions in β-position and cyclic structures with 4–7 carbon atoms. The new parameters improved the accuracy with 60% of the predicted data now lying within a range of 80% of the experimental values. The method itself is easy to handle for nonexpert users and the calculation of rate constants can be easily automatized based on the information provided in the publication. However, the method is currently restricted to H-abstraction reactions of alkanes, carboxylic acids, carboxylates and alcohols due to missing descriptors for other compound classes such as carbonyl compounds. This considerably limits the applicability of this user-friendly method.

In 2009 Minakata et al.[103] used a large database of 310 compounds to develop a group contribution method with 66 individual group rate constants and 80 group contribution factors and another 124 compounds to test their training set. 83% of their training set and 62% of the validation set were found to be within a factor of 2 of the experimental data.

Minakata and co-authors used only one group contribution factor per neighboring group as Monod et al.[28] in their first approach. However, Minakata et al.[103] reached a higher accuracy with their SAR approach than in ref. [28]. Another huge advantage is the treatment not only of H-abstraction reactions of saturated aliphatic compounds, including group contribution factors to account for cyclic structures, but also OH addition to alkenes and aromatic compounds. Group rate constants are assigned for CH_x groups as well as hydroxyl and carboxylic acid

Table 16. Compilation of newly measured aqueous phase SO_4^- radical kinetic data relevant for atmospheric chemistry. Coding and abbreviations are explained in the text or below the Table.

Reactant	Technique	pH	k_{2nd} [$M^{-1}s^{-1}$]	Comments	A [$M^{-1}s^{-1}$]	E_A [kJ mol^{-1}]	Measuring technique	Ref.
Aliphatic alcohols								
1,2-ethanediol	LFP/$S_2O_8^{2-}$	~6	$(2.7\pm0.3)\times10^7$	1	$(3.7\pm0.2)\times10^9$	12.1 ± 3.3	direct/SO_4^-/473 nm	[24]
1,2-propanediol	LFP/$S_2O_8^{2-}$	~6	$(4.3\pm0.9)\times10^7$	1	$(1.2\pm0.1)\times10^{10}$	13.8 ± 3.2	direct/SO_4^-/473 nm	[24]
1,2,3-propanetriol	LFP/$S_2O_8^{2-}$	~6	$(3.7\pm0.4)\times10^7$	1	$(3.9\pm0.3)\times10^9$	11.7 ± 4.2	direct/SO_4^-/473 nm	[24]
erythritol	LFP/$S_2O_8^{2-}$	~6	$(4.2\pm0.3)\times10^7$	1	$(2.6\pm0.1)\times10^8$	4.5 ± 1.6	direct/SO_4^-/473 nm	[24]
arabitol	LFP/$S_2O_8^{2-}$	~6	$(5.3\pm1.0)\times10^7$	1	$(3.9\pm0.4)\times10^{10}$	16.5 ± 5.4	direct/SO_4^-/473 nm	[24]
mannitol	LFP/$S_2O_8^{2-}$	~6	$(5.0\pm0.7)\times10^7$	1	$(1.6\pm0.1)\times10^{10}$	14.4 ± 4.4	direct/SO_4^-/473 nm	[24]
levoglucosan	LFP/$S_2O_8^{2-}$	~6	$(5.2\pm0.9)\times10^7$	1	$(2.1\pm0.1)\times10^9$	9 ± 3	direct/SO_4^-/473 nm	[110]
Carboxylic acids								
lactic acid	LFP/$S_2O_8^{2-}$	1	$(1.0\pm0.1)\times10^7$	1	–	–	direct/SO_4^-/407 nm	[130]
lactate	LFP/$S_2O_8^{2-}$	9	$(1.6\pm0.1)\times10^7$	1	–	–	direct/SO_4^-/407 nm	[130]
glycolic acid	LFP/$S_2O_8^{2-}$	1.5	$(4.2\pm0.4)\times10^6$	1	–	–	direct/SO_4^-/407 nm	[130]
glycolate	LFP/$S_2O_8^{2-}$	9	$(1.6\pm0.2)\times10^7$	1	–	–	direct/SO_4^-/407 nm	[130]
malic acid	LFP/$S_2O_8^{2-}$	1	$(7.7\pm0.3)\times10^6$	1	–	–	direct/SO_4^-/407 nm	[130]
malate (mono-anion)	LFP/$S_2O_8^{2-}$	4.3	$(8.5\pm0.4)\times10^6$	1	–	–	direct/SO_4^-/407 nm	[130]
malate (di-anion)	LFP/$S_2O_8^{2-}$	9	$(1.5\pm0.1)\times10^7$	1	–	–	direct/SO_4^-/407 nm	[130]
malonic acid	LFP/$S_2O_8^{2-}$	1	$(2.7\pm0.1)\times10^6$	1	–	–	direct/SO_4^-/407 nm	[130]
malonate (mono-anion)	LFP/$S_2O_8^{2-}$	4.3	$(1.5\pm0.1)\times10^6$	1	–	–	direct/SO_4^-/407 nm	[130]
malonate (di-anion)	LFP/$S_2O_8^{2-}$	9	$(5.1\pm0.4)\times10^6$	2, A, □,○	–	–	direct/SO_4^-/407 nm	[130]
oxalic acid	LFP/$S_2O_8^{2-}$	1	1.4×10^5	1	–	–	direct/SO_4^-/450 nm	[129]
	LFP/$S_2O_8^{2-}$	1	$(1.1\pm0.1)\times10^6$	1	–	–	direct/SO_4^-/407 nm	[130]
oxalate (mono-anion)	LFP/$S_2O_8^{2-}$	3	3.0×10^6	1	–	–	direct/SO_4^-/450 nm	[129]
	LFP/$S_2O_8^{2-}$	2.8	$(1.7\pm0.1)\times10^6$	1	–	–	direct/SO_4^-/407 nm	[130]
oxalate (di-anion)	LFP/$S_2O_8^{2-}$	7	5.6×10^6	1	–	–	direct/SO_4^-/450 nm	[129]
	LFP/$S_2O_8^{2-}$	9	$(1.3\pm0.1)\times10^7$	1	–	–	direct/SO_4^-/407 nm	[130]
Aromatic compounds								
ferulic acid	LFP/$S_2O_8^{2-}$		3.2×10^9	1	–	–	direct/SO_4^-/460 nm	[131]
caffeic acid	LFP/$S_2O_8^{2-}$		3.9×10^9	1	–	–	direct/SO_4^-/460 nm	[131]
sinapic acid	LFP/$S_2O_8^{2-}$		3.6×10^9	1	–	–	direct/SO_4^-/460 nm	[131]
chlorogenic acid	LFP/$S_2O_8^{2-}$		2.0×10^9	1	–	–	direct/SO_4^-/460 nm	[131]
benzene	AO of S(IV)	3	2.4×10^9	2, A*, B, □,○,●	–	–	O_2 time profiles	[99]
phenol	AO of S(IV)	3	8.8×10^9	1	–	–	O_2 time profiles	[99]
gallic acid	LFP/$S_2O_8^{2-}$		$(6.3\pm0.7)\times10^8$	1	–	–	direct/SO_4^-	[132]
gallate	LFP/$S_2O_8^{2-}$		$(2.9\pm0.2)\times10^9$	1	–	–	direct/SO_4^-	[132]
benzaldehyde	PR		0.7×10^9	1	–	–	direct/PBK	[53]
m-hydroxybenzaldehyde	PR		4.2×10^9	1	–	–	direct/PBK	[53]
p-hydroxybenzaldehyde	PR		5.9×10^9	1	–	–	direct/PBK	[53]
m-methoxybenzaldehyde	PR		0.43×10^9	1	–	–	direct/PBK	[53]
p-methoxybenzaldehyde	PR		0.8×10^9	1	–	–	direct/PBK	[53]
p-chlorobenzaldehyde	PR		2.7×10^9	1	–	–	direct/PBK	[53]
p-nitrobenzaldehyde	PR		0.45×10^9	1	–	–	direct/PBK	[53]
Other organic compounds								
dimethylsulfoxide (DMSO)	LFP/$S_2O_8^{2-}$		$(3.0\pm0.4)\times10^9$	2, A, ○	3.7×10^{11}	12.0 ± 0.4	direct/SO_4^-/445 nm	[133]
dimethylsulfone ($DMSO_2$)	LFP/$S_2O_8^{2-}$		$<(3.9\pm0.5)\times10^6$	1	5.1×10^9	11.3 ± 1.3	direct/SO_4^-/445 nm	[133]
methanesulfonate (MS)	LFP/$S_2O_8^{2-}$		$(1.1\pm0.3)\times10^4$	1	4.8×10^7	20.7 ± 4.3	direct/SO_4^-/445 nm	[133]
α-pinene	AO of S(IV)	3	1.2×10^9	2, B, ●	–	–	O_2 time profiles	[99]
myrtenal	AO of S(IV)	3	9.6×10^8	2, A, ●	–	–	O_2 time profiles	[99]
cis-pinonic acid	AO of S(IV)	3	1.6×10^7	1	–	–	O_2 time profiles	[99]
isoprene	TD/$S_2O_8^{2-}$	8–8.5	2.1×10^9	1	–	–	calculated	[134]
Inorganic compounds								
chloride anion	LFP/$S_2O_8^{2-}$		$(3.2\pm0.2)\times10^8$	2, A*, □,○,●	–	–	direct/SO_4^-/450 nm	[90]
sulphate radical	LFP/$S_2O_8^{2-}$		$(6.1\pm0.2)\times10^8$	2, A*, □,○	–	–	direct/SO_4^-/450 nm	[90]
peroxodisulphate anion	LFP/$S_2O_8^{2-}$		$(5.5\pm0.3)\times10^5$	2, A*, □,○,●	–	–	direct/SO_4^-/450 nm	[90]
water	LFP/$S_2O_8^{2-}$		$(4.6\pm0.9)\times10^2$ s^{-1}	2, A*, □,○	–	–	direct/SO_4^-/450 nm	[90]

PR = Pulse radiolysis; LFP = Laser flash photolysis; AO = Auto oxidation; □ Neta et al., 1988[4]; ○ NIST[6]; ● Herrmann, 2003[7]

functional groups. Group contribution factors are able to treat all kinds of hydrocarbons, oxygenated organic compounds, and organics substituted with sulphur, nitrogen, or phosphor species. In a second paper by the same group[104] an automated mechanism generator was introduced to predict the pathways of degradation reactions and determine byproducts for

Table 17. Summary of the available kinetic data measured for SO_4^{-} radical reactions with benzene at $T=298$ K in aqueous solution.

Technique	pH	k_{2nd} [$M^{-1}s^{-1}$]	Measuring technique	Ref.
AO of S(IV)	3	2.4×10^9		[99]
LFP/$S_2O_8^{2-}$	4	$(6.4\pm2.5)\times10^8$	direct/SO_4^{-}/442 nm	[98]
PR	7	3.0×10^9	direct/SO_4^{-}/450 nm	[97]
PR	n.r.	8.0×10^8	direct	[95]
AO of S(IV)	3	2.4×10^9	calculated	[135]

Table 18. Summary of the available kinetic data measured for SO_4^{-} radical reactions with α-pinene at $T=298$ K in aqueous solution.

Technique	pH	k_{2nd} $M^{-1}s^{-1}$	Measuring technique	Ref.
AO of S(IV)	3	1.2×10^9		[99]
PR	4	$(3.1\pm0.1)\times10^9$	direct/SO_4^{-}/450 nm	[136]

advanced oxidation reactions in aqueous solution. The model was developed based on experimental observations. The algorithm presented by Li and Crittenden[104] uses object-oriented programming. In this approach each molecule is treated as an object and reacts according to elementary reaction rules. Within the model of Li and Crittenden OH radicals react with parent molecules either by H-abstraction or addition to an unsaturated bond. The formed alkyl radicals react further with oxygen forming organic peroxy radicals. Peroxy radicals undergo uni- or bimolecular decay according to the studies of von Sonntag and Schuchman.[105] As a specialty in aqueous solution the mechanism generator treats also the hydration of carbonyl compounds and subsequent changes in the H-abstraction sites. A mechanism generator in combination with a group contribution method is a promising approach to describe aqueous phase degradation processes of radicals in aqueous solutions for a wide range of compounds. Similar tools are already available for the description of gas phase oxidation processes. However, results need to be carefully validated due to the rather complex chemistry in aqueous solution. Furthermore, effects of the hydration, protonation or the dissociation have to be included since they can change the reactivity as well as the degradation chemistry.

The SAR method presented by Minakata et al.[103] has the advantage of a much wider application range in comparison to the method presented by Monod and Doussin.[102] The wide application range in combination with the user-friendliness makes it probably the best currently available estimation tool for OH radical reactions in aqueous solution.

Wang et al.[106] developed a quantitative structure–activity relationship of OH reactions with phenols, alkanes, and alcohols using a database of 55 organic compounds. Using quantum chemical descriptors such as the energy of the highest occupied molecular orbital (E_{HOMO}), the average net charge on an H-atom ($\overline{Q_H}$), the molecular surface area, and the dipole moment (μ) good results with a R^2 of 0.905 were reached. The authors compared the performance of their model to the methods published in Monod et al.[28] and Monod and Doussin[102] and found a better agreement between the experimental and calculated values using their own method.

Another QSAR provided by Kusic et al. [107] uses 78 aromatic compounds of which 60 were used as a training set. Quantum mechanical descriptors were used to predict reaction rate constants of OH with aromatic compounds. They found that the E_{HOMO} descriptor is the most important one for the description of the degradation rates. However, different models with up to five descriptors were tried. The model with four and five descriptors gave the best results in predicting aqueous-phase OH rate constants. However, the training- and validation set of Kusic and coworkers[107] is restricted to aromatic compounds only and the applicability of their method to other classes of compounds has not been shown.

However, an implementation of the QSAR methods described by Wang et al. and Kusic et al. in atmospheric multiphase chemistry models seems unpractical at the moment since a number of quantum chemical descriptors are needed. These data are usually not available for all compounds of atmospheric interest and therefore further calculations would become necessary.

A more straightforward method for the estimation of H-abstraction rate constants of gas- and aqueous phase reactions goes back to the work of Evans and Polanyi in 1938.[108] This empirical approach correlates the bond dissociation energy (BDE) of the weakest H-bond in the molecule with the activation energy (E_A) according to the following relationship [Eq. (2)]:

$$E_A = a' + b'\mathrm{BDE(C{-}H)} \quad (2)$$

where a' and b' are coefficients of the linear regression equation. Applying the Arrhenius equation, this relationship can be extended to estimate rate constants per abstractable H-atom (k_H) given that all pre-exponential factors (A) of the considered reactions are similar, as can be seen from Equation 3:

$$\log\frac{k}{n_H} = \log k_H = \left(\log A - \frac{a'}{RT}\right) - \frac{b'}{RT}\mathrm{BDE(C-H)} \quad (3)$$

Bond dissociation energies of the organic reactants are available from laboratory and computational studies or can be calculated for many compounds with the incremental method by Benson.[109] The method of Benson allows the calculation of gas-phase bond strengths for a wide range of compound classes with an accuracy of ±8 kJ mol^{-1}. It was shown in several applications that the gas phase BDEs calculated with the method of Benson can be used for aqueous-phase Evans–Polanyi-type correlations as well. These correlations can be used for all reactions of radicals following an H-abstraction mechanism. Furthermore, Evans–Polanyi-type correlations can predict activation energies of H-abstraction reactions, which is not possible with all of the SAR methods presented before. Overall, such correlations are a useful and easy to use tool for the estimation of kinetic data for a wide range of compounds. Problems using this method arise mainly from the fact that bond

dissociation energies are not easily accessible or that other reaction mechanisms than H-abstraction contribute to the overall rate constant. Also the incremental method of Benson has some restrictions. Not all compounds can be treated with this method due to sometimes missing increments. Furthermore, neighboring effects on bond strength are not considered which can be a serious limitation for poly-functional compounds. Since the incremental method was originally developed for the calculation of gas-phase BDEs effects, the dissociation and protonation cannot be described with this method. The latest Evans–Polanyi correlation for OH radical reactions in aqueous solution is published in Hoffmann et al.,[24] and shown in Equation (4). This correlation contains 52 reactions ($n=52$) of different alcohols, carbonyls and carboxylic acids. The relatively weak correlation coefficient of $r=0.73$ and the only slightly negative slope of (0.04 ± 0.01) reflects the low selectivity of OH radicals [Eq. (4)]:

$$\log k_{H} = (24.2 \pm 4.1) - (0.04 \pm 0.01) \times \mathrm{BDE}\ [\mathrm{kJ\,mol^{-1}}] \qquad (4)$$

where $n=52$ and $r=0.73$.

In the following section Evans–Polanyi-type correlations have been used to calculate rate constants of compounds belonging to different compound classes. For these calculations separate Evans–Polanyi correlations have been established for each class of compounds considered. The corresponding data for these correlations as well as the correlation itself for each compound class can be found in the Supporting Information (Table S5).

Comparison of Different Estimation Methods

In the following the robustness of the estimation methods presented by Monod and Doussin[102] and Minakata et al.[103] is compared. When no results were available from Monod and Doussin[102] the older results from Monod et al.[28] were used for comparison. Furthermore, results from Evans–Polanyi-type correlations for each considered compound class were compared as well. The quantitative structure–activity relationships published by Wang et al.[106] and Kusic et al.[107] are not considered due to the mentioned impractical choice of input parameters. The comparison between these three methods was done for different compound classes.

Individual figures, showing estimated versus measured rate constants, for each compound class are discussed in the following. Ideally, the slope of the linear regression lines presented in Figures 6–10 should be equal to 1 and the *y*-intercept should be zero for the method to work properly.

Alkanes: In Figure 6 the methods of Monod and Doussin[102] and Minakata et al.[103] as well as Evans–Polanyi-type correlations are compared for saturated hydrocarbons. All three methods show very good agreement with the experimental data. Best agreement is reached by Minakata et al.[103] The method of Monod and Doussin[102] seems to underestimate the rate constants somewhat for longer carbon chains, but still reaches reasonable results. The Evans–Polanyi correlation for alkanes tends to slightly overestimate rate constants, in particular for the fast reactions of heptane and octane.

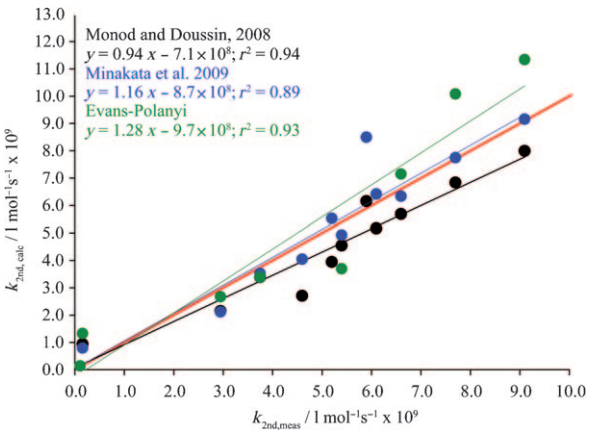

Figure 6. Comparison of experimental and estimated kinetic data (see Table S5 in the Supporting Information) for alkanes in aqueous solution applying three different prediction tools. The red line indicates the line of same reactivity.

Alcohols: The reactivity of mono-alcohols is also reasonably described by all three estimation methods (Figure 7). However, the SAR methods are more precise in comparison to the Evans–Polanyi approach if one considers all compounds in Figure 7. Problems with the calculated values using the Evans–Polanyi correlation probably arise from uncertainties in both the available bond dissociation energies and the number of abstracted H-atoms considered for the calculations. The poly-alcohols in Figure 8 show a different trend. As can be seen in Figure 8, none of the methods describes the reactivity of poly-alcohols in a reasonable manner. The results are extremely scattered and estimated kinetic data should be used with great care. The description of poly functional alcohols surely requires a further refinement.

Carboxylic Acids: The reactivity of mono- and dicarboxylic acids in Figure 9 is well described by both SAR methods. The

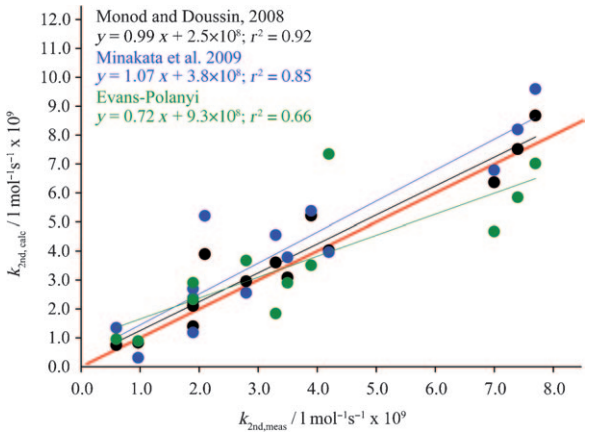

Figure 7. Comparison of experimental and estimated kinetic data (see Table S5 in the Supporting Information) for mono alcohols in aqueous solution applying three different prediction tools. The red line indicates the line of same reactivity.

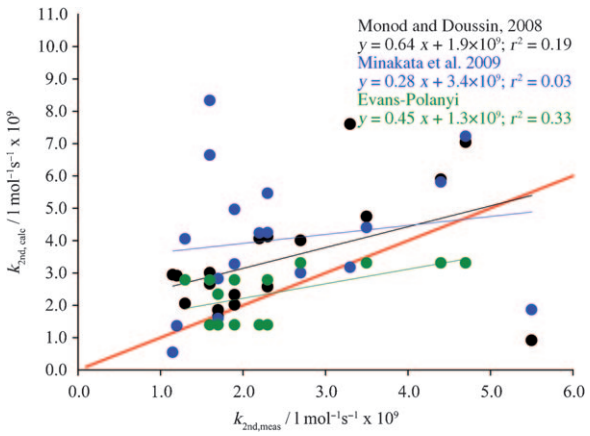

Figure 8. Comparison of experimental and estimated kinetic data (see Table S5 in the Supporting Information) for poly alcohols in aqueous solution applying three different prediction tools. The red line indicates the line of same reactivity.

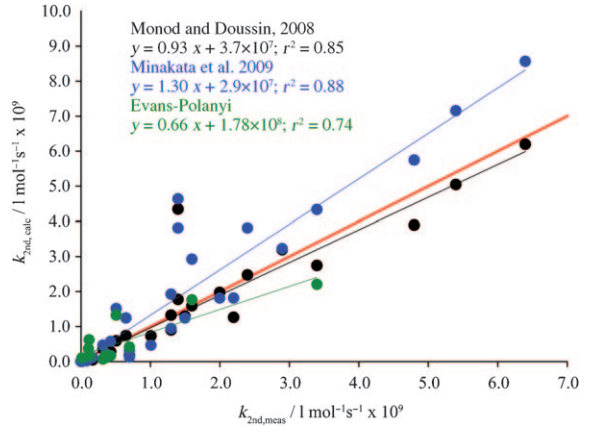

Figure 9. Comparison of experimental and estimated kinetic data (see Table S5 in the Supporting Information) for carboxylic acids in aqueous solution applying three different prediction tools. The red line indicates the line of same reactivity.

slope of both regression lines is close to 1 and the correlation coefficients are reasonable high. Again, the method by Minakata[103] seems to slightly overestimate the reactivity of carboxylic acids. Interestingly, the reactivity of dicarboxylic acids is much better described by these methods than the reactivity of poly functional alcohols. Reasons for this behavior remain unclear at this point. The quality of the Evans–Polanyi approach is hard to evaluate since most of the considered reactions show only a low reactivity. It can hardly be decided whether the Evans–Polanyi correlation can also be applied for faster reactions based on the data of Figure 9.

Carbonyl Compounds: Estimating reactivities of carbonyl compounds is not a trivial task due to the hydration of these compounds in aqueous solution. Accordingly, the robustness of the estimation methods compared in this study is much lower in comparison to other compound classes. The method presented by Monod and Doussin is currently not able to treat carbonyl compounds due to missing parameters. Therefore, the older method published by Monod and coworkers[28] was used to calculate the rate constants in Figure 10. Even if the slopes of the regression lines from both SAR methods in Figure 10 are around 1, the data points itself are so scattered

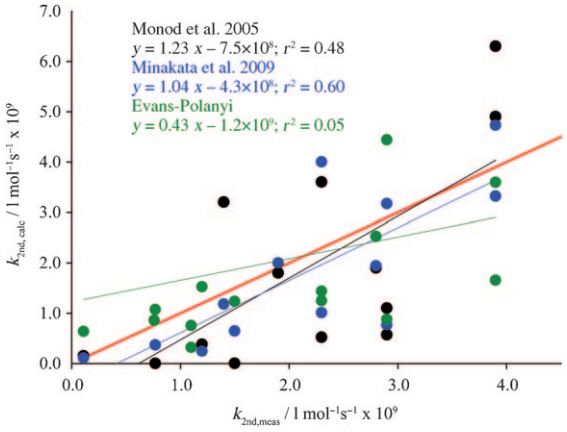

Figure 10. Comparison of experimental and estimated kinetic data (see Table S5 in the Supporting Information) for carbonyl compounds in aqueous solution applying three different prediction tools. The red line indicates the line of same reactivity.

that calculations using both methods should only be taken as a rough orientation. The Evans–Polanyi type correlation also does not work properly for this class of reactants. Calculated kinetic data applying this approach are extremely scattered and can not be used for a reliable estimation of rate constants.

A huge advantage of the method of Minakata et al.[103] is the applicability to a large variety of different species and types of reactions. Out of the three compared methods in this chapter only the approach of Minakata et al.[103] allows the calculation of OH radical rate constants with unsaturated aliphatic and aromatic compounds. Only this method can treat OH addition reactions to double bonds or aromatic ring systems. Overall, the method of Minakata et al.[103] is currently the most broadly usable method for the prediction OH radical reaction rates in aqueous solution. However, the performance of the method presented by Monod and Doussin[102] is not poorer, only the applicability is more limited. The Evans–Polanyi approach shows the weakest performance considering the whole tested data set. But, strengths of this method are its user friendliness, the possibility to predict activation energies and the applicability of this method to H-abstraction reactions of other radicals. In particular the latter point is a very important advantage since corresponding SAR methods for other atmospheric relevant free radicals in aqueous solution are fully missing at the moment. In summary, it can be stated that there are a couple of tools available to estimate OH radical kinetic data in aqueous solution as it is often needed for the modeling purposes. All of the available methods have their merits and weak points as well. The reactivity of mono functional aliphatic compounds is treated reasonably well by all methods with some restrictions for carbonyl compounds. Furthermore, it appears that es-

timations on the reactivity of poly functional compounds still contain large uncertainties and need further refinements.

5.2. NO_3 Radical

As mentioned before, SAR methods such as those existing for OH radicals in aqueous solution are still missing for the estimation of NO_3 aqueous phase kinetic data. The only currently available choice is an Evans–Polanyi-type correlation. The latest correlation for NO_3 reactions in aqueous solution contains 38 compounds and ($n=38$) was published by our group in 2009[24] [Eq. (5)]:

$$\log k_H = (39.9 \pm 5.4) - (0.087 \pm 0.014) \times \mathrm{BDE}\ [\mathrm{kJ\,mol^{-1}}] \qquad (5)$$

where $n=38$ and $r=0.90$. This correlation published by Hoffmann et al.[24] contains 38 H-abstraction reactions of aliphatic alcohols, carbonyls and carboxylic acids. The correlation coefficient of $r=0.90$ is significantly higher than the one for the OH radical correlation shown above. Furthermore, NO_3 radicals show a much higher selectivity compared to OH. The NO_3 rate constants considered in Hoffmann et al.[24] increase by approximately four orders of magnitude if one lowers the bond strengths from 410 kJ mol^{-1} to 360 kJ mol^{-1}.

5.3. SO_4^- Radical

Again the reactivity of sulphate radical anions can be only estimated using the Evans–Polanyi approach. The latest correlation with a total number of 29 compounds ($n=29$) was recently published in Hoffmann et al. in 2009[24] [Eq. (6)]:

$$\log k_H = (29.4 \pm 9.3) - (0.06 \pm 0.02) \times \mathrm{BDE}\ [\mathrm{kJ\,mol^{-1}}] \qquad (6)$$

where $n=29$ and $r=0.68$. However, the correlation is much more scattered than for NO_3 radicals even if similar compounds have been included. Reasons for this relatively weak correlation are not clear since the H-abstraction mechanism should dominate the reactions in all cases. Therefore, further measurements should be included in order to strengthen the correlation and to check the scope of application. The Evans–Polanyi plot for SO_4^- radical anions show a similar slope and intercept as observed for NO_3, which is due to the higher selectivity in comparison to OH.

6. Summary and Outlook

Herein sources, properties such as the UV absorption spectra and the kinetics of newly studied reactions of the free radicals OH, NO_3 and SO_4^- were summarized and reviewed. In a sense, this contribution is a continuation of the former reviews by Buxton et al.,[3] Neta et al.,[4] Herrmann and Zellner[5] and Herrmann.[7] With all of these together a reader can have a sensible data compilation of aqueous phase kinetic and other useful data which can lay the groundwork for a further advancement of chemical multiphase mechanisms. Most of the remeasured kinetic data presented herein are in agreement with former determinations. Larger discrepancies between novel and already published rate constants have been discussed and recommendations have been provided whenever possible. Furthermore, available data on OH quantum yields, the OH radical absorption spectra and the thiocyanate reference system in general have been reviewed and discussed. If possible, recommendations or averaged data of these parameters have been provided. These kind of information can be applied in future laboratory studies of atmospheric aqueous reactions.

Apparently, and demonstrated by the published studies, time seems to be right to do a step forward into the prediction of aqueous phase rate constants with a high demand on the precision of the predicted rate constant. A number of promising approaches is seen in this field at the time being, however, this development appears to just have started. The currently available estimation methods as well as their merits and weak points have been summarized and discussed in this contribution. While the reactivity of many monofunctional aliphatic compounds is treated reasonably well with these methods it appears that estimations on the reactivity of poly functional compounds contain still larger uncertainties. Furthermore, generally applicable prediction tools which cover also other atmospheric oxidants, reaction products and reaction mechanisms are still missing or under construction. Better prediction tools will allow one to set up more complex particle-phase chemical schemes which are beyond what is available at current and preferably should cover three bulk compartments that are coupled together: the gas phase, the aqueous phase and the organic phase. Needless to say that it is expected that there will be additional complex chemical conversions and interaction at all the interfaces involved.

The development of better prediction tools for the condensed phase and here aqueous phase chemistry in the troposphere will be a big advancement but it will still be accompanied by further detailed laboratory kinetic investigation which are preparing the ground for even better prediction tools in the future. Such advance in knowledge and step to better understand the tropospheric multiphase system, finally up to the level of its predictability, can only be based on sound laboratory work and the establishment of firm rules from a data set enabling this.

Acknowledgements

The authors and especially H.H. are pleased to dedicate this contribution to Philippe Mirabel, Robert Lesclaux and Georges LeBras from whom we have learned a lot over the years. These three friends have contributed enormously to form the community of atmospheric chemists throughout Europe and beyond. We would like to thank Luisa Schöne for her help with this manuscript. Funding enabling systematic work on aqueous phase chemistry of atmospheric relevance is gratefully acknowledged from DFG (projects MISOX (HE 3086/13-1) and ACETOX (HE 3086/8-1)) and the EC via ACCENT (GOCE-CT-2004-505337).

Keywords: atmospheric chemistry · kinetics · radicals · reactivity · spectroscopic methods

[1] A. Tilgner, H. Herrmann, *Atmos. Environ.* **2010**, DOI: doi:10.1016/j.atmosenv.2010.07.050.
[2] H. Herrmann, A. Tilgner, P. Barzaghi, Z. Majdik, S. Gligorovski, L. Poulain, A. Monod, *Atmos. Environ.* **2005**, *39*, 4351 – 4363.
[3] G. V. Buxton, C. L. Greenstock, W. P. Helman, A. B. Ross, *J. Phys. Chem. Ref. Data* **1988**, *17*, 513 – 886.
[4] P. Neta, R. E. Huie, A. B. Ross, *J. Phys. Chem. Ref. Data* **1988**, *17*, 1027 – 1284.
[5] H. Herrmann, R. Zellner in *N-centered Radicals* (Eds. Z. B. Alfassi), Wiley, New York, **1998**, pp. 291 – 343.
[6] *NIST Solution Kinetics Database Version 3.0*, Gaithersburg, **1998**.
[7] H. Herrmann, *Chem. Rev.* **2003**, *103*, 4691 – 4716.
[8] R. Wolke, A. M. Sehili, M. Simmel, O. Knoth, A. Tilgner, H. Herrmann, *Atmos. Environ.* **2005**, *39*, 4375 – 4388.
[9] L. Deguillaume, M. Leriche, K. Desboeufs, G. Mailhot, C. George, N. Chaumerliac, *Chem. Rev.* **2005**, *105*, 3388 – 3431.
[10] M. Leriche, D. Voisin, N. Chaumerliac, A. Monod, B. Aumont, *Atmos. Environ.* **2000**, *34*, 5015 – 5036.
[11] L. Deguillaume, M. Leriche, A. Monod, N. Chaumerliac, *Atmos. Chem. Phys.* **2004**, *4*, 95 – 110.
[12] H. Herrmann, *Phys. Chem. Chem. Phys.* **2007**, *9*, 3935 – 3964.
[13] X. Y. Yu, J. R. Barker, *J. Phys. Chem. A* **2003**, *107*, 1325 – 1332.
[14] D. E. Lea, *Trans. Faraday Soc.* **1949**, *45*, 81 – 85.
[15] F. S. Dainton, J. Rowbottom, *Trans. Faraday Soc.* **1953**, *49*, 1160 – 1173.
[16] M. Hatada, I. Kraljic, A. Elsamahy, C. N. Trumbore, *J. Phys. Chem.* **1974**, *78*, 888 – 891.
[17] B. G. Kwon, J. H. Kwon, *J. Ind. Eng. Chem.* **2010**, *16*, 193 – 199.
[18] J. K. Thomas, J. Rabani, M. S. Matheson, E. J. Hart, S. Gordon, *J. Phys. Chem.* **1966**, *70*, 2409 – 2410.
[19] E. Janata, *Proc. Indian Acad. Sci. Chem. Sci.* **2002**, *114*, 731 – 737.
[20] M. S. Alam, E. Janata, *Chem. Phys. Lett.* **2006**, *417*, 363 – 366.
[21] H. Christensen, K. Sehested, *Radiat. Phys. Chem.* **1981**, *18*, 723 – 731.
[22] A. J. Elliot, G. V. Buxton, *J. Chem. Soc. Faraday Trans.* **1992**, *88*, 2465 – 2470.
[23] D. M. Chipman, *J. Phys. Chem. A* **2008**, *112*, 13372 – 13381.
[24] D. Hoffmann, B. Weigert, P. Barzaghi, H. Herrmann, *Phys. Chem. Chem. Phys.* **2009**, *11*, 9351 – 9363.
[25] M. S. Alam, B. S. M. Rao, E. Janata, *Rad. Phys. Chem.* **2003**, *67*, 723 – 728.
[26] S. Gligorovski, D. Rousse, C. H. George, H. Herrmann, *Int. J. Chem. Kinet.* **2009**, *41*, 309 – 326.
[27] T. Moise, Y. Rudich, D. Rousse, C. George, *Environ. Sci. Technol.* **2005**, *39*, 5203 – 5208.
[28] A. Monod, L. Poulain, S. Grubert, D. Voisin, H. Wortham, *Atmos. Environ.* **2005**, *39*, 7667 – 7688.
[29] S. P. Mezyk, D. R. Hardison, W. H. Song, K. E. O'Shea, D. M. Bartels, W. J. Cooper, *Chemosphere* **2009**, *77*, 1352 – 1357.
[30] H. Bardouki, M. B. da Rosa, N. Mihalopoulos, W. U. Palm, C. Zetzsch, *Atmos. Environ.* **2002**, *36*, 4627 – 4634.
[31] L. Zhu, J. M. Nicovich, P. . Wine, *Aquat. Sci.* **2003**, *65*, 425 – 435.
[32] B. G. Ershov, E. Janata, M. S. Alam, A. V. Gordeev, *High Energy Chem.* **2008**, *42*, 1 – 6.
[33] L. R. Martin, S. P. Mezyk, B. J. Mincher, *J. Phys. Chem. A* **2009**, *113*, 141 – 145.
[34] N. Getoff, F. Schworer, V. M. Markovic, K. Sehested, S. O. Nielsen, *J. Phys. Chem.* **1971**, *75*, 749 – 755.
[35] Z. D. Draganic, M. M. Kosanic, I. G. Draganic, *J. Phys. Chem.* **1964**, *68*, 2085 – 2092.
[36] B. Ervens, S. Gligorovski, H. Herrmann, *Phys. Chem. Chem. Phys.* **2003**, *5*, 1811 – 1824.
[37] M. N. Schuchmann, H. P. Schuchmann, M. Hess, C. von Sonntag, *J. Am. Chem. Soc.* **1991**, *113*, 6934 – 6937.
[38] D. Volgger, A. J. Zemann, G. K. Bonn, M. J. Antal, *J. Chromatogr. A* **1997**, *758*, 263 – 276.
[39] I. Morozov, S. Gligorovski, P. Barzaghi, D. Hoffmann, Y. G. Lazarou, E. Vasiliev, H. Herrmann, *Int. J. Chem. Kinet.* **2008**, *40*, 174 – 188.
[40] S. P. Mezyk, T. Helgeson, S. K. Cole, W. J. Cooper, R. V. Fox, P. R. Gardinali, B. J. Mincher, *J. Phys. Chem. A* **2006**, *110*, 2176 – 2180.
[41] B. H. Milosavljevic, J. A. LaVerne, S. M. Pimblott, *J. Phys. Chem. A* **2005**, *109*, 7751 – 7756.
[42] C. Walling, G. M. El-Taliawi, R. A. Johnson, *J. Am. Chem. Soc.* **1974**, *96*, 133 – 139.
[43] Z. B. Alfassi, G. I. Khaikin, R. D. Johnson, P. Neta, *J. Phys. Chem.* **1996**, *100*, 15961 – 15967.
[44] M. C. Facchini, S. Decesari, M. Rinaldi, C. Carbone, E. Finessi, M. Mircea, S. Fuzzi, F. Moretti, E. Tagliavini, D. Ceburnis, C. D. O'Dowd, *Environ. Sci. Technol.* **2008**, *42*, 9116 – 9121.
[45] C. Müller, Y. Iinuma, J. Karstensen, D. van Pinxteren, S. Lehmann, T. Gnauk, H. Herrmann, *Atmos. Chem. Phys.* **2009**, *9*, 9587 – 9597.
[46] J. N. Smith, K. C. Barsanti, H. R. Friedli, M. Ehn, M. Kulmala, D. R. Collins, J. H. Scheckman, B. J. Williams, P. H. McMurry, *Proc. Natl. Acad. Sci. USA* **2010**, *107*, 6634 – 6639.
[47] S. P. Mezyk, D. B. Ewing, J. J. Kiddle, K. P. Madden, *J. Phys. Chem. A* **2006**, *110*, 4732 – 4737.
[48] R. Zona, S. Solar, N. Getoff, K. Sehested, J. Holcman, *Rad. Phys. Chem.* **2010**, *79*, 626 – 636.
[49] B. G. Kwon, S. Ryu, J. Yoon, *J. Ind. Eng. Chem.* **2009**, *15*, 809 – 812.
[50] F. S. García Einschlag, L. Carlos, A. L. Capparelli, *Chemosphere* **2003**, *53*, 1 – 7.
[51] M. S. Elovitz, H. Shemer, J. R. Peller, K. Vinodgopal, M. Sivaganesan, K. G. Linden, *J. Water Supply Res. Technol. AQUA* **2008**, *57*, 391 – 401.
[52] I. E. Makarov, E. L. Protasova, G. I. Khaikin, *Russ. J. Phys. Chem. A* **2008**, *82*, 1833 – 1837.
[53] S. Geeta, B. S. M. Rao, H. Mohan, J. P. Mittal, *J. Phys. Org. Chem.* **2004**, *17*, 194 – 198.
[54] C. B. Amphlett, G. E. Adams, B. D. Michael, *Adv. Chem. Ser.* **1968**, *81*, 231 – 250.
[55] R. S. Shetiya, K. N. Rao, J. Shankar, *Indian J. Chem. Sect. A* **1976**, *14*, 575 – 578.
[56] P. Neta, L. M. Dorfman, *Adv. Chem. Ser.* **1968**, *81*, 222 – 230.
[57] Q. G. Mulazzani, G. V. Buxton, *Chem. Phys. Lett.* **2006**, *421*, 261 – 265.
[58] B. H. Milosavljevic, J. A. LaVerne, *J. Phys. Chem. A* **2005**, *109*, 165 – 168.
[59] R. Zellner, H. Herrmann, in *Advances in Spectroscopy* (Eds. R. J. H. Clark, R. E. Hester), Wiley, Chichester, **1995**, pp. 381 – 451.
[60] D. Zehavi, J. Rabani, *J. Phys. Chem.* **1972**, *76*, 312 – 319.
[61] M. S. Matheson, W. A. Mulac, J. L. Weeks, J. Rabani, *J. Phys. Chem.* **1966**, *70*, 2092 – 2099.
[62] M. Chin, P. H. Wine, *J. Photochem. Photobiol. A* **1992**, *69*, 17 – 25.
[63] A. J. Elliot, A. S. Simsons, *Rad. Phys. Chem.* **1984**, *24*, 229 – 231.
[64] G. E. Adams, J. W. Boag, B. D. Michael, *Trans. Faraday Soc.* **1965**, *61*, 1417 – 1424.
[65] J. H. Baxendale, D. A. Stott, *J. Chem. Soc. Chem. Commun.* **1967**, 699 – 700.
[66] J. H. Baxendale, P. L. T. Bevan, D. A. Stott, *Trans. Faraday Soc.* **1968**, *64*, 2389 – 2397.
[67] D. H. Ellison, G. A. Salmon, F. Wilkinson, *Proc. R. Soc. London Ser. A* **1972**, *328*, 23 – 36.
[68] D. Behar, P. L. T. Bevan, G. Scholes, *J. Phys. Chem.* **1972**, *76*, 1537 – 1542.
[69] G. Z. Wu, Y. Katsumura, Y. Muroya, M. Z. Lin, T. Morioka, *J. Phys. Chem. A* **2001**, *105*, 4933 – 4939.
[70] L. Dogliotti, E. Hayon, *J. Phys. Chem.* **1968**, *72*, 1800 – 1807.
[71] A. Iwata, N. Nakashima, M. Kusaba, Y. Izawa, C. Yamanaka, *Chem. Phys. Lett.* **1993**, *207*, 137 – 142.
[72] M. C. Sauer, R. A. Crowell, I. A. Shkrob, *J. Phys. Chem. A* **2004**, *108*, 5490 – 5502.
[73] G. E. Adams, J. W. Boag, J. Currant, B. D. Michael in *Pulse Radiolysis of Aqueous Solutions of Thiocyanate Ions* (Eds. M. Ebert, J. P. Keene, A. J. Swallow, J. H. Baxendale), Academic Press, London, **1965**, pp. 117 – 129.
[74] G. E. Adams, J. W. Boag, B. D. Michael, *Trans. Faraday Soc.* **1965**, *61*, 1674 – 1680.
[75] P. Caregnato, S. G. Bertolotti, M. C. Gonzalez, D. O. Martire, *Photochem. Photobiol.* **2005**, *81*, 1526 – 1533.
[76] G. Czapski, J. Holcman, B. H. J. Bielski, *J. Am. Chem. Soc.* **1994**, *116*, 11465 – 11469.

[77] R. P. Wayne, I. Barnes, P. Biggs, J. P. Burrows, C. E. Canosamas, J. Hjorth, G. Lebras, G. K. Moortgat, D. Perner, G. Poulet, G. Restelli, H. Sidebottom, *Atmos. Environ.* **1991**, *25*, 1 – 203.
[78] Y. Rudich, R. K. Talukdar, A. R. Ravishankara, *J. Geophys. Res. [Atmos.]* **1996**, *101*, 21 023 – 21 031.
[79] M. Schütze, H. Herrmann, *J. Atmos. Chem.* **2005**, *52*, 1 – 18.
[80] T. Umschlag, R. Zellner, H. Herrmann, *Phys. Chem. Chem. Phys.* **2002**, *4*, 2975 – 2982.
[81] P. Barzaghi, H. Herrmann, *Phys. Chem. Chem. Phys.* **2004**, *6*, 5379 – 5388.
[82] P. G. de Semainville, D. Hoffmann, C. George, H. Herrmann, *Phys. Chem. Chem. Phys.* **2007**, *9*, 958 – 968.
[83] C. Weller, D. Hoffmann, T. Schaefer, H. Herrmann, *Z. Phys. Chem.* **2010**, *224*, 1261 – 1287.
[84] D. M. Stanbury, *Adv. Inorg. Chem.* **1989**, *33*, 69 – 138.
[85] O. Ito, S. Akiho, M. Iino, *Bull. Chem. Soc. Jpn.* **1989**, *62*, 1606 – 1611.
[86] A. K. Pikaev, G. Sibirska, E. M. Shirshov, P. Y. Glazunov, V. I. Spit *syn, Dokl. Akad. Nauk SSSR* **1974**, *215*, 645 – 648.
[87] E. Hayon, A. Treinin, J. Wilf, *J. Am. Chem. Soc.* **1972**, *94*, 47 – 57.
[88] H. Herrmann, B. Ervens, H. W. Jacobi, R. Wolke, P. Nowacki, R. Zellner, *J. Atmos. Chem.* **2000**, *36*, 231 – 284.
[89] W. J. McElroy, S. J. Waygood, *J. Chem. Soc. Faraday Trans.* **1990**, *86*, 2557 – 2564.
[90] X. Y. Yu, Z. C. Bao, J. R. Barker, *J. Phys. Chem. A* **2004**, *108*, 295 – 308.
[91] J. Criquet, N. K. V. Leitner, *Chemosphere* **2009**, *77*, 194 – 200.
[92] L. Dogliotti, E. Hayon, *J. Phys. Chem.* **1967**, *71*, 2511 – 2516.
[93] E. Heckel, A. Henglein, G. Beck, *Ber. Bunsen-Ges.* **1966**, *70*, 149 – 154.
[94] B. Lesigne, C. Ferradin, J. Pucheaul, *J. Phys. Chem.* **1973**, *77*, 2156 – 2158.
[95] W. Roebke, M. Renz, A. Henglein, *Int. J. Radiat. Phys. Chem.* **1969**, *1*, 39 – 44.
[96] O. P. Chawla, R. W. Fessenden, *J. Phys. Chem.* **1975**, *79*, 2693 – 2700.
[97] P. Neta, V. Madhavan, H. Zemel, R. W. Fessenden, *J. Am. Chem. Soc.* **1977**, *99*, 163 – 164.
[98] H. Herrmann, H. Exner, W. Jacobi, G. Raabe, A. Reese, R. Zellner, *Faraday Discuss.* **1995**, *100*, 129 – 153.
[99] J. Ziajka, W. Pasiuk-Bronikowska, *Atmos. Environ.* **2005**, *39*, 1431 – 1438.
[100] R. Atkinson, *Int. J. Chem. Kinet.* **1987**, *19*, 799 – 828.
[101] E. S. C. Kwok, R. Atkinson, *Atmos. Environ.* **1995**, *29*, 1685 – 1695.
[102] A. Monod, J. F. Doussin, *Atmos. Environ.* **2008**, *42*, 7611 – 7622.
[103] D. Minakata, K. Li, P. Westerhoff, J. Crittenden, *Environ. Sci. Technol.* **2009**, *43*, 6220 – 6227.
[104] K. Li, J. Crittenden, *Environ. Sci. Technol.* **2009**, *43*, 2831 – 2837.
[105] C. von Sonntag, H.-P. Schuchmann in *Peroxy Radicals* (Eds. Z. B. Alfassi), Wiley, Chichester, **1997**, pp. 173 – 234.
[106] Y. N. Wang, J. W. Chen, X. H. Li, S. Y. Zhang, X. L. Qiao, *QSAR Comb. Sci.* **2009**, *28*, 1309 – 1316.
[107] H. Kušić, B. Rasulev, D. Leszczynska, J. Leszczynski, N. Koprivanac, *Chemosphere* **2009**, *75*, 1128 – 1134.
[108] M. G. Evans, M. Polanyi, *Trans. Faraday Soc.* **1938**, *34*, 11 – 24.
[109] S. W. Benson, *Thermochemical Kinetics*, Wiley, New York, **1976**.
[110] D. Hoffmann, A. Tilgner, Y. Iinuma, H. Herrmann, *Environ. Sci. Technol.* **2010**, *44*, 694 – 699.
[111] J. A. Williams, W. J. Cooper, S. P. Mezyk, D. M. Bartels, *Rad. Phys. Chem.* **2002**, *65*, 327 – 334.
[112] D. R. Hardison, W. J. Cooper, S. P. Mezyk, D. M. Bartels, *Rad. Phys. Chem.* **2002**, *65*, 309 – 315.
[113] X. Y. Yu, J. R. Barker, *J. Phys. Chem. A* **2003**, *107*, 1313 – 1324.
[114] L. Ashton, G. V. Buxton, C. R. Stuart, *J. Chem. Soc. Faraday Trans.* **1995**, *91*, 1631 – 1633.
[115] B. S. Wolfenden, R. L. Willson, *J. Chem. Soc. Perkin Trans. 2* **1982**, 805 – 812.
[116] H. Cohen, D. Meyerstein, *J. Am. Chem. Soc.* **1971**, *93*, 4179 – 4183.
[117] R. L. Willson, C. L. Greenstock, G. E. Adams, R. Wageman, L. M. Dorfman, *Int. J. Radiat. Phys. Chem.* **1971**, *3*, 211 – 220.
[118] R. F. Anderson, K. B. Patel, M. R. L. Stratford, *J. Chem. Soc. Faraday Trans. 1* **1987**, *83*, 3177 – 3187.
[119] R. J. Field, N. V. Raghavan, J. G. Brummer, *J. Phys. Chem.* **1982**, *86*, 2443 – 2449.
[120] E. J. Land, M. Ebert, *Trans. Faraday Soc.* **1967**, *63*, 1181 – 1190.
[121] D. Zehavi, J. Rabani, *J. Phys. Chem.* **1971**, *75*, 1738 – 1744.
[122] M. Tanaka, H. Sakuma, O. Kohanawa, S. Fukaya, M. Katayama, *Bull. Chem. Soc. Jpn.* **1984**, *57*, 3403 – 3407.
[123] N. Motohashi, Y. Saito, *Chem. Pharm. Bull.* **1993**, *41*, 1842 – 1845.
[124] M. Chin, P. H. Wine in *Aquatic and Surface Photochemistry* (Eds. G. Helz, G. Zepp, D. G. Crosby), Lewis Publishers, Boca Raton, **1994**, pp. 85 – 96.
[125] S. V. Lymar, H. A. Schwarz, G. Czapski, *Rad. Phys. Chem.* **2000**, *59*, 387 – 392.
[126] G. Nord, B. Pedersen, E. Floryanlovborg, P. Pagsberg, *Inorg. Chem.* **1982**, *21*, 2327 – 2330.
[127] D. Rousse, C. George, *Phys. Chem. Chem. Phys.* **2004**, *6*, 3408 – 3414.
[128] P. G. de Sémainville, B. D'Anna, C. George, *Z. Phys. Chem.* **2010**, *224*, 1247 – 1260.
[129] X. K. Yang, J. Q. Wang, T. D. Wang, *Chin. Chem. Lett.* **2004**, *15*, 583 – 586.
[130] I. Grgić, B. Podkrajšek, P. Barzaghi, H. Herrmann, *Atmos. Environ.* **2007**, *41*, 9187 – 9194.
[131] H. P. Zhu, H. W. Zhao, Z. X. Zhang, W. F. Wang, S. D. Yao, *Radiat. Environ. Biophys.* **2006**, *45*, 73 – 77.
[132] P. Caregnato, P. M. D. Gara, G. N. Bosio, M. C. Gonzalez, N. Russo, M. D. C. Michelini, D. O. Martire, *J. Phys. Chem. A* **2008**, *112*, 1188 – 1194.
[133] L. Zhu, J. M. Nicovich, P. H. Wine, *J. Photochem. Photobiol. A* **2003**, *157*, 311 – 319.
[134] K. J. Rudzinski, *J. Atmos. Chem.* **2004**, *48*, 191 – 216.
[135] P. Warneck, J. Ziajka, *Ber. Bunsen-Ges.* **1995**, *99*, 59 – 65.
[136] G. V. Buxton, G. A. Salmon, J. E. Williams, *J. Atmos. Chem.* **2000**, *36*, 111 – 134.
[137] J. P. Hunt, H. Taube, *J. Am. Chem. Soc.* **1952**, *74*, 5999 – 6002.
[138] J. L. Weeks, M. S. Matheson, *J. Am. Chem. Soc.* **1956**, *78*, 1273 – 1278.
[139] J. H. Baxendale, J. A. Wilson, *Trans. Faraday Soc.* **1957**, *53*, 344.
[140] D. H. Volman, J. C. Chen, *J. Am. Chem. Soc.* **1959**, *81*, 4141 – 4144.
[141] M. Daniels, *J. Phys. Chem.* **1962**, *66*, 1473 – 1477.
[142] G. V. Buxton, W. K. Wilmarth, *J. Phys. Chem.* **1963**, *67*, 2835 – 2841.
[143] A. Schäfer, *Ph.D. Thesis*, University of Mainz (Germany), **1991**.
[144] L. Sun, J. R. Bolton, *J. Phys. Chem.* **1996**, *100*, 4127 – 4134.
[145] L. Chu, C. Anastasio, *J. Phys. Chem. A* **2005**, *109*, 6264 – 6271.
[146] I. Nicole, J. De Laat, M. Dore, J. P. Duguet, C. Bonnel, *Water Res.* **1990**, *24*, 157 – 168.
[147] G. A. Loraine, W. H. Glaze, *J. Adv. Oxid. Technol.* **1999**, *4*, 424 – 433.
[148] R. A. Crowell, R. Lian, M. C., Jr. Sauer, D. A. Oulianov, I. A. Shkrob, *Chem. Phys. Lett.* **2004**, *383*, 481 – 485.
[149] S. Goldstein, D. Aschengrau, Y. Diamant, J. Rabani, *Environ. Sci. Technol.* **2007**, *41*, 7486 – 7490.
[150] I. Janik, D. M. Bartels, C. D. Jonah, *J. Phys. Chem. A* **2007**, *111*, 1835 – 1843.
[151] J. W. Boyle, J. A. Ghormley, C. J. Hochanadel, J. F. Riley, *J. Phys. Chem.* **1969**, *73*, 2886 – 2890.
[152] J. Hesper, *Ph.D. Thesis*, University of Leipzig (Germany), **2003**.
[153] P. Pagsberg, H. Christensen, J. Rabani, G. Nilsson, J. Fenger, S. O. Nielsen, *J. Phys. Chem.* **1969**, *73*, 1029 – 1038.
[154] C. L. Thomsen, D. Madsen, J. A. Poulsen, J. Thøgersen, S. J. Knak Jensen, S. R. Keiding, *J. Chem. Phys.* **2001**, *115*, 9361 – 9369.
[155] S. O. Nielsen, B. D. Micheal, E. J. Hart, *J. Phys. Chem.* **1976**, *80*, 2482 – 2488.
[156] G. G. Jayson, B. J. Parsons, A. J. Swallow, *J. Chem. Soc. Faraday Trans. 1* **1973**, *69*, 1597 – 1607.
[157] G. Czapski, B. H. J. Bielski, *Radiat. Phys. Chem.* **1993**, *41*, 503 – 505.
[158] R. H. Schuler, L. K. Patterson, E. Janata, *J. Phys. Chem.* **1980**, *84*, 2088 – 2089.
[159] G. V. Buxton, G. A. Salmon, N. D. Wood, *A Contribution to Subproject HALIPP, The Proceedings of EUROTRAC Symposium 90*, SPB Academic Publishing, **1991**, 303 – 305.
[160] G. V. Buxton, S. McGowan, G. A. Salmon, J. E. Williams, N. D. Wood, *Atmos. Environ.* **1996**, *30*, 2483 – 2493.
[161] E. Hayon, J. J. McGarvey, *J. Phys. Chem.* **1967**, *71*, 1472 – 1477.
[162] K. L. Ivanov, E. M. Glebov, V. F. Plyusnin, Y. V. Ivanov, V. P. Grivin, N. M. Bazhin, *J. Photochem. Photobiol. A* **2000**, *133*, 99 – 104.
[163] P. Y. Jiang, Y. Katsumura, R. Nagaishi, M. Domae, K. Ishikawa, K. Ishigure, Y. J. Yoshida, *J. Chem. Soc. Faraday Trans.* **1992**, *88*, 1653 – 1658.
[164] H. Schuchmann, D. J. Deeble, G. Olbrich, C. von Sonntag, *Int. J. Radiat. Biol.* **1987**, *51*, 441 – 453.

[165] Y. Tang, R. P. Thorn, R. L. Mauldin, P. H. Wine, *J. Photochem. Photobiol. A* **1988**, *44*, 243 – 258.
[166] B. G. Ershov, A. I. Mustafae, A. K. Pikaev, *Int. J. Radiat. Phys. Chem.* **1971**, *3*, 71 – 84.
[167] S. C. Choure, M. M. M. Bamatraf, B. S. M. Rao, R. Das, H. Mohan, J. P. Mittal, *J. Phys. Chem. A* **1997**, *101*, 9837 – 9845.
[168] G. Merga, B. S. M. Rao, R. Das, H. Mohan, J. P. Mittal, *J. Phys. Chem.* **1994**, *98*, 9158 – 9164.

Received: July 2, 2010
Published online on November 30, 2010

